

City size and the spreading of COVID-19 in Brazil

Haroldo V. Ribeiro,^{1,*} Andre S. Sunahara,¹ Jack Sutton,² Matjaž Perc,^{3,4,5} and Quentin S. Hanley²

¹*Departamento de Física, Universidade Estadual de Maringá – Maringá, PR 87020-900, Brazil*

²*School of Science and Technology, Nottingham Trent University,
Clifton Lane, Nottingham NG11 8NS, United Kingdom*

³*Faculty of Natural Sciences and Mathematics, University of Maribor, Koroška cesta 160, 2000 Maribor, Slovenia*

⁴*Department of Medical Research, China Medical University Hospital, China Medical University, Taichung, Taiwan*

⁵*Complexity Science Hub Vienna, Josefstädterstraße 39, 1080 Vienna, Austria*

(Dated: November 3, 2021)

The current outbreak of the coronavirus disease 2019 (COVID-19) is an unprecedented example of how fast an infectious disease can spread around the globe (especially in urban areas) and the enormous impact it causes on public health and socio-economic activities. Despite the recent surge of investigations about different aspects of the COVID-19 pandemic, we still know little about the effects of city size on the propagation of this disease in urban areas. Here we investigate how the number of cases and deaths by COVID-19 scale with the population of Brazilian cities. Our results indicate small towns are proportionally more affected by COVID-19 during the initial spread of the disease, such that the cumulative numbers of cases and deaths *per capita* initially decrease with population size. However, during the long-term course of the pandemic, this urban advantage vanishes and large cities start to exhibit higher incidence of cases and deaths, such that every 1% rise in population is associated with a 0.14% increase in the number of fatalities *per capita* after about four months since the first two daily deaths. We argue that these patterns may be related to the existence of proportionally more health infrastructure in the largest cities and a lower proportion of older adults in large urban areas. We also find the initial growth rate of cases and deaths to be higher in large cities; however, these growth rates tend to decrease in large cities and to increase in small ones over time.

INTRODUCTION

Human activities have become increasingly concentrated in urban areas. A direct consequence of this worldwide urbanization process is that more people are living in cities than in rural regions since 2007 [1], and projections indicate that the world urban population could reach more than 90% by the end of this century [2]. Besides being increasingly urbanized, we live in an unprecedentedly connected, and highly mobile world with air passengers exceeding 4 billion in 2018 [3]. On the one hand, a highly connected and highly urbanized society brought us innovation, economic growth, more access to education and healthcare; on the other, it has also led to pollution, environmental degradation, privacy concerns, more people living in substandard conditions, and suitable conditions for dissemination of infectious diseases over the globe. In particular, the emergence of infectious disease outbreaks has significantly increased over time, and the majority of these events are caused by pathogens originating in wildlife [4], which in turn has been associated with changes in environmental conditions and land use, agricultural practices, and the rise of large human population settlements [5].

The ongoing outbreak of the novel coronavirus (SARS-CoV-2) seems to fit well the previous context as it was first identified in Wuhan in December 2019, an influential Chinese city exceeding 11 million inhabitants, and

apparently originated from the recombination of bat and Malayan pangolin coronaviruses [6]. The coronavirus disease 2019 (COVID-19) initially spread in Mainland China but rapidly caused outbreaks in other countries, making the World Health Organization first declare a “Public Health Emergency of International Concern” in January 2020, and in mid-March, the outbreak was reclassified as a pandemic. As of 16 August 2020, over 21.2 million cases of COVID-19 have been confirmed in almost all countries, and the worldwide death toll exceeds 761 thousand people [7]. The COVID-19 pandemic poses unprecedented health and economic threats to our society, and understanding its spreading patterns may find important factors for mitigating or controlling the outbreak.

Recent works have focused on modeling the initial spreading of COVID-19 [8] or the fatality curves [9], projecting the outbreak peak and hospital utilization [10], understanding the effects of mobility [11], demography [12], travel restrictions [13], behavior change on the virus transmission [14], mitigation strategies [15], non-pharmaceutical interventions [16], network-based strategies for social distancing [17], among many others. Despite the increasing surge of scientific investigations on the subject, little attention has been paid to understanding the effects of city size on spreading patterns of cases and deaths by COVID-19 in urban areas. The idea that size (as measured by population) affects different city indicators has been extensively studied and can be summarized by the urban scaling hypothesis [18–21]. This theory states that urban indicators are nonlinearly associated with city population such that socio-economic indicators tend to present increasing returns

* hvr@dfi.uem.br

to scale [18, 22, 23], infrastructure indicators often display economy of scale [18, 19], and quantities related to individual needs usually scale linearly with city population [18, 19].

Urban scaling studies of health-related quantities have shown that the incidence and mortality of diseases are non-linearly related to the city population [24–27]. Despite the existence of several exceptions [27], noninfectious diseases (such as diabetes) are usually less prevalent in large cities, while infectious diseases (such as AIDS) are relatively more common in large urban areas. This different behavior is likely to reflect the fact that people living in large cities tend to have proportionally more contacts and a higher degree of social interactions than those living in small towns [19, 28]. Within this context, the recent work of Stier, Berman, and Bettencourt [29] has indicated that large cities in the United States experienced more pronounced growth rates of COVID-19 cases during the first weeks after the introduction of the disease. Similarly, Cardoso and Gonçalves [30] found that the *per capita* contact rate of COVID-19 increases with the size and density of cities in United States, Brazil and Germany. These findings have serious consequences for the evolution of COVID-19 and suggest that large metropolises may become infection hubs with potentially higher and earlier peaks of infected people. Investigating whether this behavior generalizes to other places and how different quantities such as the number of cases and deaths scale with city size are thus important elements for a better understanding of the spreading of COVID-19 in urban areas.

Here we investigate how population size is associated with cases and deaths by COVID-19 in Brazilian cities. Brazil is the sixth most populous country in the world, with over 211 million people, of which more than 85% live in urban areas. While it is likely that the novel coronavirus was already circulating in Brazil in early February 2020 [31], the first confirmed case in the country dates back to 26 February 2020, in the city of São Paulo. Between the first case and 12 August 2020, Brazil has confirmed 3,088,670 cases of COVID-19 (second-largest number) spread out over 98.9% of the 5,570 Brazilian cities. This disease caused 102,817 deaths (second-largest number) with 3,892 cities reporting at least one casualty as of 12 August 2020.

RESULTS

We start by briefly presenting our data set (see Methods for details). Our investigations rely on the daily reports published by the Health Offices of each of the 27 Brazilian federative units. These daily reports update the number of confirmed cases (Y_c) and the number of deaths (Y_d) caused by COVID-19 in every Brazilian city from 25 February 2020 (date of the first case in Brazil) to 12 August 2020 (date of our last update). From these data, we create time series of the number of cases $Y_c(t_c)$

for each city, where t_c refers to the number of days since the first two daily cases reported in each city. Similarly, we create time series of the number of deaths $Y_d(t_d)$, where t_d refers to the number of days since the first two daily deaths reported in each city. By doing so, we group all cities according to their stage of disease propagation (as measured by t_c or t_d) to investigate the evolution of allometric relationships between total cases or deaths and city population. We have also considered different number of daily cases or deaths as the reference point, and our results are robust against different choices (from one to seven daily cases or daily deaths, see Figures 1-14 in S1 Appendix).

Figure 1A shows the relation between cases of COVID-19 and city population on a logarithmic scale ($\log Y_c$ versus $\log P$) for different numbers of days since the first two daily cases ($t_c = 15, 58, 101$ and 141 days). The approximately linear behavior on logarithmic scale indicates that the number of cases is well described by a power-law function of the city population

$$Y_c \sim P^{\beta_c}, \quad (1)$$

where β_c is the so-called urban scaling exponent [18]. Similarly, Figure 1B shows the association between the number of casualties and the city population on logarithmic scale ($\log Y_d$ versus $\log P$) for different numbers of days since two daily deaths first reported ($t_d = 15, 50, 85$ and 120 days). Again, the results indicate that the number of deaths is approximated by a power-function of the city population

$$Y_d \sim P^{\beta_d}, \quad (2)$$

where β_d represents the urban scaling exponent for the number of deaths.

The results of Figure 1 also show the adjusted allometric relationships (dashed lines) and the best fitting scaling exponents β_c and β_d (see Methods for details). These exponents exhibit an increasing trend with time so that β_c and β_d exceed one after some number of days after the first two daily cases or deaths. This dynamic behavior is better visualized in Figure 2, where we depict β_c and β_d as a function of the number of days since the first two daily cases (t_c) or deaths (t_d). The scaling exponent for the number of cases β_c is sub-linear ($\beta_c < 1$) during the first four months and appears to approach a super-linear plateau ($\beta_c > 1$) as the number of days t_c further increases. The dynamic behavior of the scaling exponent for deaths β_d is similar to β_c ; however, β_d appears to be approaching a plateau larger than the one observed for β_c .

The evolution of the scaling exponents for cases and deaths indicates that small cities are proportionally more affected by COVID-19 during the first four months. However, this initial apparent advantage of living in large cities vanishes with time, and become a disadvantage after about four months. This is more evident by estimating the number of cases *per capita* from Eq. (1), that is,

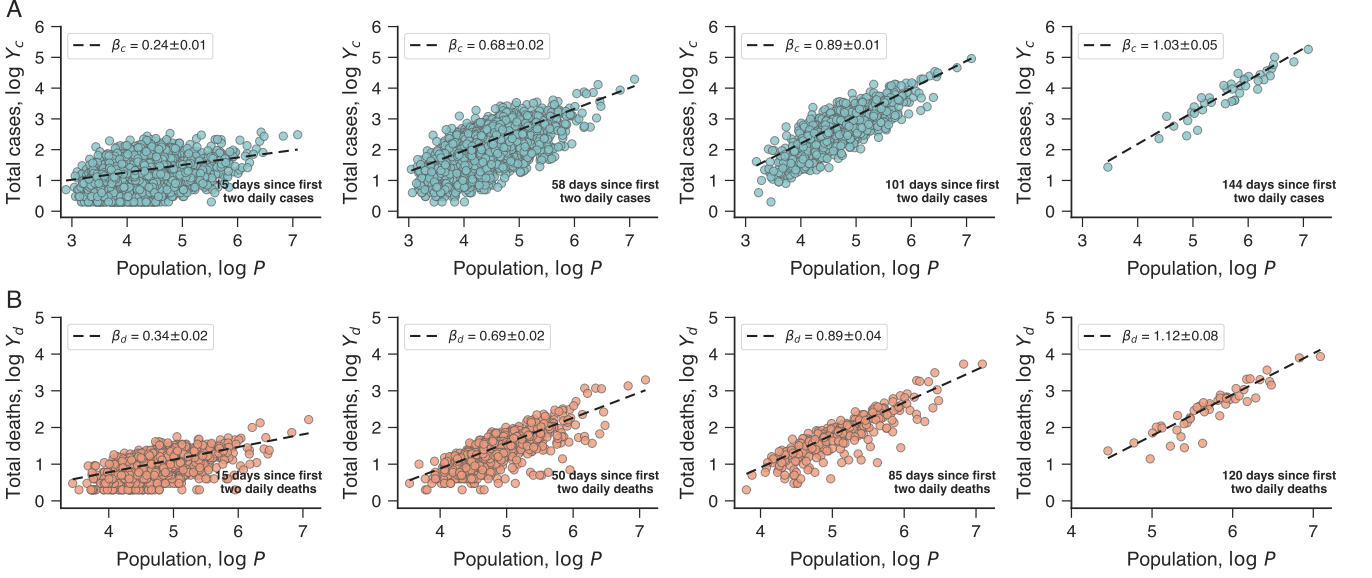


FIG. 1. **Urban scaling relations of COVID-19 cases and deaths.** (A) Relationship between the total of confirmed cases of COVID-19 (Y_c) and city population (P) on logarithmic scale. Panels show scaling relations for the number of cases on a particular day after the first two daily cases reported in each city (four evenly spaced values of t_c between 15 days and the largest value yielding at least 50 cities, as indicated within panels). (B) Relationship between the total of deaths caused by COVID-19 (Y_d) and population (P) of Brazilian cities (on logarithmic scale). Panels show scaling relations for the number of deaths on a particular day after the first two daily deaths reported in each city (four evenly spaced values of t_d between 15 days and the largest value yielding at least 50 cities, as indicated within panels). In all panels, the markers represent cities and the dashed lines are the adjusted scaling relations with best-fitting exponents indicated in each plot (β_c for cases and β_d for deaths).

$Y_c/P \sim P^{\beta_c-1}$. Similarly, we can estimate the number of deaths *per capita* from Eq. (2), yielding $Y_d/P \sim P^{\beta_d-1}$. Thus, we expect the number of COVID-19 cases or deaths *per capita* to decrease with the city population if $\beta_c < 1$ and $\beta_d < 1$; conversely, these *per capita* numbers are expected to increase with the city population if $\beta_c > 1$ and $\beta_d > 1$. For instance, because $\beta_c \approx 0.77$ and $\beta_d \approx 0.85$ after 75 days since the first two daily cases or deaths, the number of cases and deaths *per capita* decreases with population as $Y_c/P \sim P^{-0.23}$ and $Y_d/P \sim P^{-0.15}$. At those particular values of t_c and t_d , a 1% rise in the population is associated with a $\approx 0.23\%$ decrease in the incidence of COVID-19 cases and $\approx 0.15\%$ reduction in the incidence of deaths. In a concrete example for $t_c = t_d = 75$ days, we expect a metropolis such as São Paulo (with ≈ 12 million people) to have $\approx 54\%$ less cases and $\approx 39\%$ less deaths *per capita* than a medium-sized city such as Maringá/PR (with ≈ 420 thousand people, $\approx 1/30$ of São Paulo), which in turn is expected to have $\approx 41\%$ less cases and $\approx 29\%$ less deaths *per capita* than a small-sized city such as Paranaíba/MS (with ≈ 42 thousand people, $\approx 1/10$ of Maringá).

However, both scaling exponents increase with time, such that this urban advantage vanishes and become a disadvantage during the long course of the pandemic. By considering our latest estimates for the scaling exponents, we find $\beta_c \approx 1.04$ ($t_c = 144$ days) and $\beta_d \approx 1.12$ ($t_d = 120$ days). Thus, at these particular values of t_c and

t_d , we expect the number of cases *per capita* to slightly increase with population ($Y_c/P \sim P^{0.04}$) and the number of fatalities *per capita* to increase with population as $Y_d/P \sim P^{0.12}$. Thus, for $\beta_d \approx 1.12$ at $t_d = 120$ days, we expect a metropolis such as São Paulo (≈ 12 million people) to have $\approx 50\%$ more deaths *per capita* than Maringá/PR (≈ 420 thousand people), which in turn is expected to have $\approx 32\%$ more deaths *per capita* than Paranaíba/MS (≈ 42 thousand people). Figures 8-14 in S1 Appendix show that the scaling relations for number of cases and deaths *per capita* support the previous discussions.

The latest estimates of β_c found for cases of COVID-19 are smaller than those reported for the 2009 H1N1 Pandemic in Brazil ($\beta_c \approx 1.2$) and HIV in Brazil and United States ($\beta_c \approx 1.4$) [27]. Similarly to what we observe for the cases of COVID-19, the allometric exponent for HIV cases in Brazil was initially sub-linear during the 1980s, became super-linear after the 1990s, and started to approach a super-linear plateau after the 2000s [27]. However, the evolution of the allometry for HIV has been much slower than what we have observed for the COVID-19. Another interesting point reported by Rocha, Thorson, and Lambiotte [27] is that the number of H1N1 cases in Brazil started to scale linearly with city population in 2010 (one year after the first outbreak). These authors also argue that this reduction in the scaling exponent possibly reflects a better response for the spread of H1N1 after the pandemic outbreak. If the behavior ob-

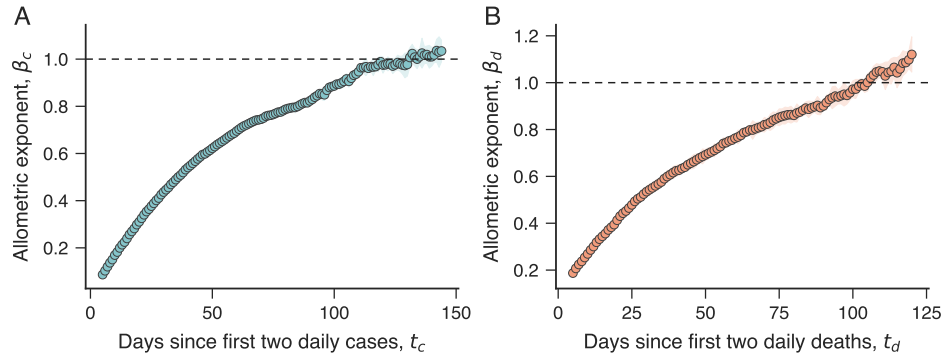


FIG. 2. **Time dependence of the scaling exponents for COVID-19 cases and deaths.** (A) Dependence of the exponent β_c on the number of days after the first two daily cases of COVID-19 (t_c). (B) Dependence of the exponent β_d on the number of days after the first two daily deaths caused by COVID-19 (t_d). The shaded regions in all panels represent bootstrap standard errors, and the horizontal dashed lines indicate the isometric scaling ($\beta_c = \beta_d = 1$). We note that β_c and β_d increase with time and appear to approach asymptotic values larger than one.

served in the 2009 H1N1 Pandemic generalizes (at least in part) for the current COVID-19 pandemic, we would expect a decrease in values of β_c in the future. The latest estimates of β_d for COVID-19 deaths are larger than those reported for diabetes ($\beta_d \approx 0.8$), heart attack ($\beta_d \approx 1$) and cerebrovascular accident ($\beta_d \approx 1$) in Brazil after the 2000s [27]. Conversely, scaling exponents related to disease mortality in Brazil displayed a decreasing trend with time, and values as high as 1.25 were observed for diabetes in 1996 ($\beta_d \approx 1.22$) and heart attack in 1981 ($\beta_d \approx 1.25$) [27]. The convergence of these exponents to linear or sub-linear regimes may reflect the increasing access to medical facilities in urban areas [27].

Based on currently available data (Figure 2), it is hard to confidently assert whether the values of β_c and β_d will remain larger than one during the long-term course of the pandemic. However, the persistence of this behavior indicates large cities are likely to be more affected at the end of the COVID-19 outbreak. Part of this behavior may be due to large cities testing for COVID-19 proportionally more than small ones. Results for the United States indicate that more rural states have lower testing rates and detect disproportionately fewer cases of COVID-19 [32]. As Brazilian cities are likely to suffer from this bias, we would expect a decrease in the scaling exponent β_c after the observed increasing trend depending on the magnitude of this effect (that is, as small cities increase their testing capabilities, their number of cases tend to increase and bend the scaling law downwards).

On the other hand, it is clearer that large cities were proportionately less affected during the initial months (since the first two daily cases or deaths) of the pandemic. We believe there are at least two possible explanations for this behavior. First, it may reflect an “increasing urban advantage” where the larger the city, the more access to medical facilities and so the chance of receiving more appropriate treatment against the coronavirus disease. A second cause can be associated with age demographic changes with the city population; specifi-

cally, a smaller proportion of older adults at high risk for severe illness and death from COVID-19 leads to a reduced number of deaths *per capita*. Another possibility is that the strategies and policy responses of large and small cities to COVID-19 are different, which in turn may lead to different efficiency in containing the pandemic. These responses are highly heterogeneous at the national level [33, 34] as well as among counties in the United States [35]. Among these three possibilities, we did not explore the possible effects of different city strategies against the COVID-19, but in light of the findings for the United States [35], this effect is likely to play an important role in the Brazilian case and may deserve further investigation.

To test for an increasing urban advantage for the treatment of COVID-19 during the initial spread of the disease, we investigate the scaling relation between the number of hospital intensive care unit (ICU) beds and city population. Because critically ill patients frequently require mechanical ventilation [36, 37], the number of ICU beds has proved to be crucial for the treatment of COVID-19. Figure 3A shows the allometric relationship between the number of ICU beds from private and public health systems (Y_{icu} , as of April 2020) and the population, where a super-linear relationship emerges with scaling exponent $\beta_{icu} \approx 1.16$. The super-linear scaling of ICU beds indicates that large Brazilian cities are better structured to deal with critically ill patients, which in turn may partially explain the reduction of deaths *per capita* with the city size during the initial three-four months since the first two daily deaths. It is worth noting that the Brazilian Public Unified Health System (Sistema Único de Saúde – SUS) is decentralized and composed of “health regions”, contiguous groups of cities usually formed by a large city and its neighboring cities [38]. Cities within the same health region may share medical services, which may in turn partially explain the reduction of the structural advantages of large urban areas

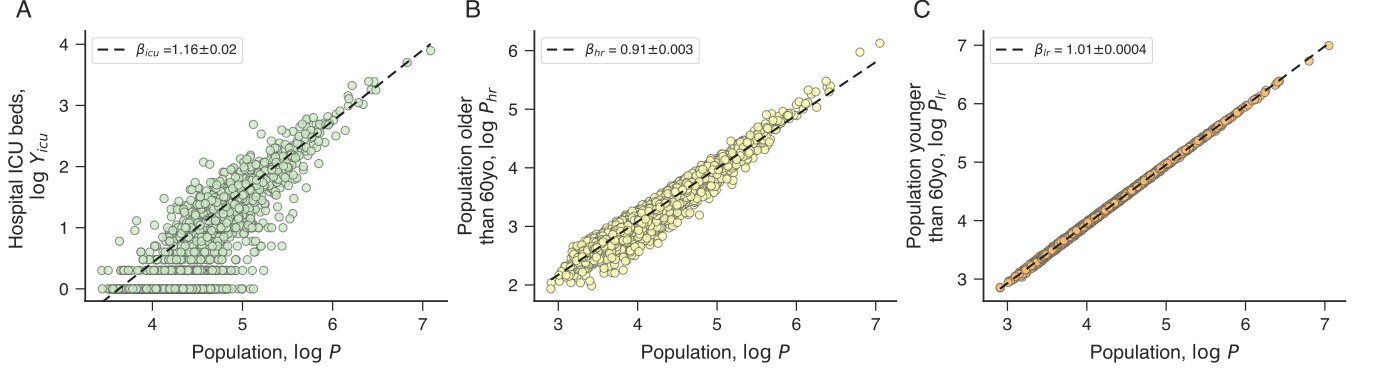


FIG. 3. Urban scaling of ICU beds, high-risk and low-risk populations. (A) Relationship between the number of ICU beds (Y_{icu}) and the city population (P) on logarithmic scale. We observe that the number of ICU beds scales super-linearly with city size ($\beta_{icu} = 1.16 \pm 0.02$), indicating an urban advantage for health coverage. (B) Relationship between the high-risk population (P_{hr} , defined as adults older than 60 years) and the city population (P) on logarithmic scale. The high-risk population scales sub-linearly ($\beta_{hr} = 0.91 \pm 0.003$), showing that large cities tend to have smaller fractions of elderly than small cities. (C) Relationship between low-risk population (P_{lr} , defined as adults younger than 60 years) and the city population (P) on logarithmic scale. We note that the low-risk population scales almost linearly ($\beta_{lr} = 1.0100 \pm 0.0004$) with city size. The behavior of these three quantities partially explains the initial decrease of number of deaths *per capita* with population ($\beta_d < 1$ for $t_d \lesssim 100$ days). See Figure 15 in S1 Appendix for the scaling relations involving *per capita* quantities.

during the long-term course of the pandemic.

We have also investigated how age demographic distribution changes with city population. Estimates have shown that the case fatality rate of COVID-19 is substantially higher in people aged more than 60 years (0.32% for those younger than 60 years versus 6.5% for those older than 60 years [39]). Thus, the age demographic of cities represents an important factor for the number of deaths caused by COVID-19. Figures 3B and 3C show how the number of people older (P_{hr} , the high-risk population) and younger (P_{lr} , the low-risk population) than 60 years change with the total population (P). We note that the high-risk population increases sub-linearly with city size with an exponent $\beta_{hr} \approx 0.91$, while the low-risk population scales linearly ($\beta_{lr} \approx 1$) with city size. This result shows that large cities have a lower prevalence of adults older than 60 years, such that a 1% increase in city population is associated with a 0.91% rise in the high-risk population. In a more concrete example, we expect a city with one million people to have proportionally $\approx 19\%$ fewer adults older than 60 years when compared with a city of 100 thousand inhabitants. Thus, a low prevalence of elderly in large urban areas may also partially explain the initial reduction of the number of deaths *per capita* with the increase of city population.

In addition to addressing the urban scaling of cases and deaths of COVID-19, we have investigated associations between the growth rates of cases and deaths and the city population (Figures 16-22 in S1 Appendix). As mentioned, the work of Stier, Berman, and Bettencourt [29] shows that the initial growth rates of COVID-19 cases in metropolitan areas of the United States scale as a power-law function of the population with an exponent between 0.11 and 0.20. By using our data and as detailed in Meth-

ods, we have estimated the growth rates of cases (r_c) and deaths (r_d) for Brazilian cities. In agreement with the United States case, our results also indicate that COVID-19 cases initially grow faster in large cities (Figure 23 in S1 Appendix), such that $r_c \sim P^{\beta_{r_c}}$ with β_{r_c} between ≈ 0.1 and ≈ 0.3 during the first three months ($t_c \lesssim 90$, Figure 23 in S1 Appendix). We also found similar behavior for the growth rate in the number of deaths r_d , where a power-law relation $r_d \sim P^{\beta_{r_d}}$ is a reasonable description for the empirical data with a scaling exponent β_{r_d} between ≈ 0.1 and ≈ 0.5 during the first three months ($t_d \lesssim 90$, Figure 23 in S1 Appendix).

The growth rate depicts a more instantaneous picture of the COVID-19 spreading process, and its association with size may change during the long-term evolution of the pandemic. These changes may reflect the different actions taken by each city to face the COVID-19 pandemic and other particularities affecting the COVID-19 spreading. For the spreading of COVID-19 in the United States, Heroy [40] has reported that large cities appear to enter in an exponential spreading regime earlier than small ones. To better investigate these possibilities in our data, we have estimated the average relationship between the growth rate of cases (r_c) and deaths (r_d) and the city rank s ($s = 1$ represents the largest city in data, $s = 2$ the second-largest, and so on) at different periods. Figure 4A shows the results for the growth rates in the number of cases (r_c). In agreement with the power-law association between r_c and the city population (Figures 16-22 in S1 Appendix), we note that lower values of the city rank s are associated with higher growth rates r_c in the initial days since the first two daily cases. However, as time goes by, the growth rate of cases starts to decrease in large cities (low-rank values) and to increase

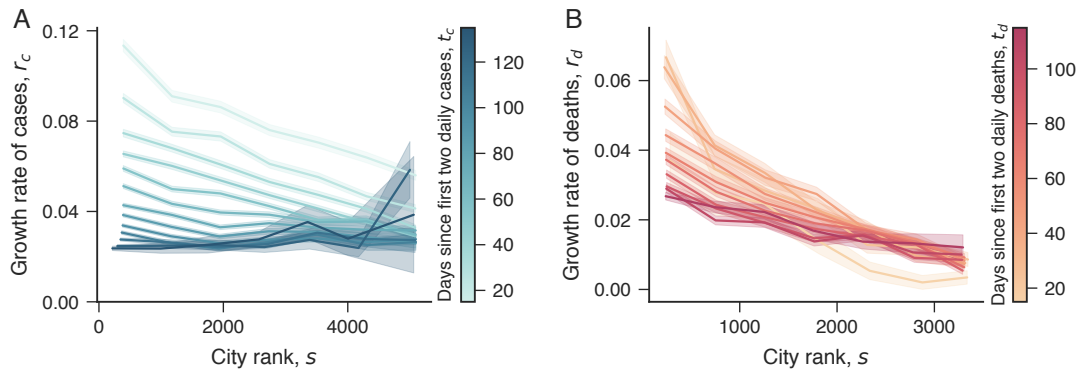


FIG. 4. **Association between growth rates and city size.** (A) Relationship between the growth rate of COVID-19 cases (r_c) and the city rank (s). The different curves show the average values r_c versus s for different number of days since the first two daily cases (t_c , as indicated by the color code). (B) Relationship between the growth rate of deaths by COVID-19 (r_d) and the city rank (s). The different curves show the average values r_d versus s for different number of days since the first two daily deaths (t_d , as indicated by the color code).

in small ones (high-rank values). This result appears to agree with the findings of Heroy [40] in the sense that there is a delay in the emergence of high growth rates of cases between large and small cities. Figure 4B shows the same analysis for growth rate in the number of deaths r_d . While we also observe a decrease in r_d for large cities and increase for small ones, the differences in r_d are less pronounced than in r_c . These findings also emerge when investigating the scaling exponents associated with the growth rates of cases (β_{r_c}) and deaths (β_{r_d}). The results of Figure 23 in S1 Appendix show that these exponents start to decrease around $t_c \approx t_d \approx 100$ days and become negative in our latest estimates. It is worth remembering that the time t_c (or t_d) is measured in days since the first two daily cases (or first two daily deaths) for each city; thus, the results of Figure 4 do not reflect delays in the emergence of the first case in each city.

DISCUSSION

We have studied scaling relations for the number of COVID-19 cases and deaths in Brazilian cities. Similarly to what happens for other diseases, we found the number of cases and deaths to be power-law related to the city population. During the initial three-four months since the first two daily cases or deaths, we found a sub-linear association between cases and deaths by COVID-19, meaning that the *per capita* numbers of cases and deaths tend to decrease with population in this initial stage of the pandemic. We believe this behavior can be partially explained by an “increasing urban advantage” where large cities have proportionally more ICU beds than small ones. In addition, changes in age demography with city size show that large cities have proportionally less elderly people who are at high risk of developing severe illness and dying from COVID-19. This may also partially explain the initial reduction of fatalities *per*

capita with the city population. In addition, we have argued that the strategies and policy responses of large and small cities to COVID-19 may also be different and lead to different efficiency in containing the pandemic.

However, we found that this “urban advantage” vanishes in the long-term course of the pandemic, such that the association between cases and deaths by COVID-19 with population becomes super-linear in our latest estimates since the first two daily cases or deaths. Thus, the persistence of this pattern indicates that large cities are expected to be proportionally more affected at the end of the COVID-19 pandemic. This result is in line with the findings for other infectious diseases [25, 27] and probably reflects the existence of a higher degree of interaction between people in large cities [19, 28]. Because social distancing is currently the only available measure to mitigate the impact of COVID-19, our results suggest that large cities may require more severe degrees of social distancing policies.

In agreement with the results for metropolitan areas in the United States [29], we have found that large cities usually display higher growth rates in the number of cases during the initial spread of the COVID-19. However, our results also show that these growth rates tend to decrease in large cities and to increase in small ones in the long-term course of the pandemic. This behavior suggests the existence of a delay in the emergence of high growth rates between large and small cities. Similar behavior was also found in the United States [40], where large cities appear to enter an exponential growth regime earlier than small towns. The existence of this delay suggests that the initial slow-spreading pace of the COVID-19 in small cities is likely to be a transient behavior.

Together with the recent findings of Stier-Berman-Bettencourt [29] and Heroy [40] for the United States, as well as those of Cardoso and Gonçalves [30] for United States, Brazil and Germany, our results suggest that social distancing policies and other actions against the pan-

demic should take into account the non-linear effects of city size on the spreading of the COVID-19.

METHODS

Data

The primary data set used in this work was collected from the `brasil.io` API [41]. This API retrieves information from COVID-19 daily reports published by the Health Offices of each of the 27 Brazilian federations (26 states and one federation district) and makes it freely available. This data set comprises information about the cumulative number of cases and deaths of COVID-19 from 25 February 2020 (date of the first case in Brazil) until 12 August 2020 (date of our last update) for all Brazilian cities reporting at least one case of COVID-19. The `brasil.io` API also provides population data of Brazilian cities, which in turn relies on population estimates for the year 2019 released by the Brazilian Institute of Geography and Statistics (IBGE). There is a total of 5,507 Brazilian cities with at least one reported case of COVID-19 on 12 August 2020, corresponding to 98.9% of the country's total number of cities. In addition, 3,892 cities suffered casualties from this disease, representing 69.9% of the total. To ensure that our estimates rely on at least 50 cities, we consider a suitable upper threshold for the time series length (Figure 24 in S1 Appendix). The data about age demographics refer to the latest Brazilian census that took place in 2010, while the data about the number of ICU beds are from April 2020. These two data sets are maintained and made freely available by the Department of Informatics of the Brazilian Public Health System (DATASUS) [42].

Fitting urban scaling laws

Urban scaling [18] usually refers to a power-law association between a city property Y and the city population P , and it is expressed by

$$Y = Y_0 P^\beta, \quad (3)$$

where Y_0 is a constant and β is the urban scaling exponent. Equation (3) can be linearized by taking the logarithmic on both sides, that is,

$$\log Y = \log Y_0 + \beta \log P, \quad (4)$$

where $\log Y$ and $\log P$ are the dependent and independent variables of the corresponding linear relationship between $\log Y$ and $\log P$. We have estimated the power-law exponents in Eq. (3) by using the probabilistic approach of Leitão *et al.* [43]. Specifically, we have found the probabilistic model with lognormal fluctuations and where the fluctuations in $\log Y$ are independent of P to be the best description of our data in the majority of scaling laws.

Thus, we assume these lognormal fluctuations in all adjusting procedures in order to estimate the values of β . It is worth mentioning that this maximum-likelihood estimate for scaling exponents is analogous to the one obtained via usual least-squares with the log-transformed variables ($\log Y$ versus $\log P$).

Logarithmic growth rates of cases and deaths

Let us consider that x_t ($t = 1, \dots, n$) represents the cumulative number of cases (Y_c) or the cumulative number of deaths (Y_d) for COVID-19 in a given city at time t (number of days since first case t_c or death t_d). The logarithmic growth rate r_t at time t is defined as

$$r_t = \log(x_t/x_{t-\tau})/\tau \quad (t = \tau, \tau + 1, \dots, n) \quad (5)$$

where τ is a time delay. If we assume the numbers of cases or deaths to initially increase exponentially ($x_t \sim e^{rt}$, where r is the exponential growth rate), r_t represents an estimate for the growth rate of this initial exponential behavior (r). We have estimated r_t for the number of cases (r_c) and deaths (r_d) up to values of t_c and t_d ensuring a sample size of at least 50 cities for the allometric relations between these growth rates and the city population (Figure 24 in S1 Appendix). All results in the main text were obtained for $\tau = 14$ but our discussion is robust for τ between 9 and 21 days (Figures 25-38 in S1 Appendix).

ACKNOWLEDGEMENTS

This research was supported by Coordenação de Aperfeiçoamento de Pessoal de Nível Superior (CAPES) and Conselho Nacional de Desenvolvimento Científico e Tecnológico (CNPq). H.V.R. thanks for the financial support of CNPq (Grant Nos. 407690/2018-2 and 303121/2018-1). M.P. acknowledges financial support of the Slovenian Research Agency (Grant Nos. J4-9302, J1-9112, and P1-0403).

DATA AVAILABILITY

All data supporting the findings of this study are freely available as detailed in the main text.

AUTHOR CONTRIBUTIONS STATEMENT

H.V.R., A.S.S., J.S., M.P., and Q.S.H. designed research, performed research, analyzed data, and wrote the paper.

ADDITIONAL INFORMATION

Competing interests: The authors declare that they have no conflict of interest.

S1 APPENDIX

Supplementary Figures (1-38) supporting the robustness of our findings against different reference points

for synchronizing the time series of cases and deaths among cities, different time delays used for estimating the growth rates, and other additional figures.

-
- [1] United Nations, World Urbanization Prospects: Urban population (% of total). Available: <http://data.worldbank.org/indicator/SP.URB.TOTL.IN.ZS>. Accessed: 27 May 2020.
 - [2] Jiang, L. & O'Neill, B. C. Global urbanization projections for the Shared Socioeconomic Pathways. *Global Environ. Chang.* **42**, 193–199 (2017).
 - [3] International Civil Aviation Organization, Civil Aviation Statistics of the World and ICAO staff estimates. Available: <https://data.worldbank.org/indicator/IS.AIR.PSGR>. Accessed: 27 May 2020.
 - [4] Jones, K. E. *et al.* Global trends in emerging infectious diseases. *Nature* **451**, 990–993 (2008).
 - [5] Wolfe, N. D., Dunavan, C. P. & Diamond, J. Origins of major human infectious diseases. *Nature* **447**, 279–283 (2007).
 - [6] Xiao, K. *et al.* Isolation of SARS-CoV-2-related coronavirus from Malayan pangolins. *Nature* **583**, 286–289 (2020).
 - [7] World Health Organization, Coronavirus disease (COVID-19) Situation Report - 209. Available: https://www.who.int/docs/default-source/coronaviruse/situation-reports/20200816-covid-19-sitrep-209.pdf?sfvrsn=5dde1ca2_2. Accessed: 19 Aug 2020.
 - [8] Maier, B. F. & Brockmann, D. Effective containment explains subexponential growth in recent confirmed COVID-19 cases in China. *Science* **368**, 742–746 (2020).
 - [9] Vasconcelos, G. L. *et al.* Modelling fatality curves of COVID-19 and the effectiveness of intervention strategies. *medRxiv* (2020). URL <https://www.medrxiv.org/content/early/2020/04/14/2020.04.02.20051557>.
 - [10] Moghadas, S. M. *et al.* Projecting hospital utilization during the COVID-19 outbreaks in the United States. *Proceedings of the National Academy of Sciences* **117**, 9122–9126 (2020).
 - [11] Gatto, M. *et al.* Spread and dynamics of the COVID-19 epidemic in Italy: Effects of emergency containment measures. *Proceedings of the National Academy of Sciences* **117**, 10484–10491 (2020).
 - [12] Dowd, J. B. *et al.* Demographic science aids in understanding the spread and fatality rates of COVID-19. *Proceedings of the National Academy of Sciences* **117**, 9696–9698 (2020).
 - [13] Chinazzi, M. *et al.* The effect of travel restrictions on the spread of the 2019 novel coronavirus (COVID-19) outbreak. *Science* **368**, 395–400 (2020).
 - [14] West, R., Michie, S., Rubin, G. J. & Amlôt, R. Applying principles of behaviour change to reduce SARS-CoV-2 transmission. *Nature Human Behaviour* **4**, 451–459 (2020).
 - [15] Walker, P. G. *et al.* The impact of COVID-19 and strategies for mitigation and suppression in low-and middle-income countries. *Science* **369**, 413–422 (2020).
 - [16] Flaxman, S. *et al.* Estimating the effects of non-pharmaceutical interventions on COVID-19 in Europe. *Nature* **584**, 257–261 (2020).
 - [17] Block, P. *et al.* Social network-based distancing strategies to flatten the COVID-19 curve in a post-lockdown world. *Nature Human Behaviour* **4**, 588–596 (2020).
 - [18] Bettencourt, L. M. A., Lobo, J., Helbing, D., Kühnert, C. & West, G. B. Growth, innovation, scaling, and the pace of life in cities. *Proceedings of the National Academy of Sciences* **104**, 7301–7306 (2007).
 - [19] Bettencourt, L. M. The origins of scaling in cities. *Science* **340**, 1438–1441 (2013).
 - [20] Batty, M. *The New Science of Cities* (MIT Press, Cambridge, MA, 2013).
 - [21] West, G. B. *Scale: The Universal Laws of Growth, Innovation, Sustainability, and the Pace of Life in Organisms, Cities, Economies, and Companies* (Penguin, New York, 2017).
 - [22] Youn, H. *et al.* Scaling and universality in urban economic diversification. *Journal of The Royal Society Interface* **13**, 20150937 (2016).
 - [23] Gao, J., Zhang, Y.-C. & Zhou, T. Computational socioeconomics. *Physics Reports* **817**, 1–104 (2019).
 - [24] Acuna-Soto, R., Viboud, C. & Chowell, G. Influenza and pneumonia mortality in 66 large cities in the United States in years surrounding the 1918 pandemic. *PLoS One* **6**, e23467 (2011).
 - [25] Antonio, F. J., de Picoli Jr, S., Teixeira, J. J. V. & dos Santos Mendes, R. Growth patterns and scaling laws governing AIDS epidemic in Brazilian cities. *PLoS ONE* **9**, e111015 (2014).
 - [26] Melo, H. P. M., Moreira, A. A., Batista, É., Makse, H. A. & Andrade, J. S. Statistical signs of social influence on suicides. *Scientific Reports* **4**, 1–6 (2014).
 - [27] Rocha, L. E., Thorson, A. E. & Lambiotte, R. The non-linear health consequences of living in larger cities. *Journal of Urban Health* **92**, 785–799 (2015).
 - [28] Schlöpfer, M. *et al.* The scaling of human interactions with city size. *Journal of the Royal Society Interface* **11**, 20130789 (2014).
 - [29] Stier, A. J., Berman, M. G. & Bettencourt, L. COVID-19 attack rate increases with city size. *arXiv:2003.10376* (2020).

- [30] Cardoso, B.-H. F. & Gonçalves, S. Urban scaling of COVID-19 epidemics. *arXiv:2005.07791* (2020).
- [31] Delatorre, E., Mir, D., Graf, T. & Bello, G. Tracking the onset date of the community spread of SARS-CoV-2 in Western Countries. *medRxiv* (2020).
- [32] Souch, J. M. & Cossman, J. S. A commentary on rural-urban disparities in COVID-19 testing rates per 100,000 and risk factors. *The Journal of Rural Health* (2020).
- [33] Hsiang, S. *et al.* The effect of large-scale anti-contagion policies on the COVID-19 pandemic. *Nature* **584**, 262–267 (2020).
- [34] Gao, J., Yin, Y., Jones, B. F. & Wang, D. Quantifying policy responses to a global emergency: Insights from the COVID-19 pandemic. *arXiv:2006.13853* (2020).
- [35] Brandtner, C., Bettencourt, L., Stier, A. & Berman, M. G. Creatures of the state? Metropolitan counties compensated for state inaction in initial US response to COVID-19 pandemic. *Mansueto Institute for Urban Innovation Research Paper* (2020).
- [36] Grasselli, G., Pesenti, A. & Cecconi, M. Critical care utilization for the COVID-19 outbreak in Lombardy, Italy: Early experience and forecast during an emergency response. *JAMA* **323**, 1545–1546 (2020).
- [37] Arabi, Y. M., Murthy, S. & Webb, S. COVID-19: A novel coronavirus and a novel challenge for critical care. *Intensive Care Medicine* **46**, 833–836 (2020).
- [38] Castro, M. C. *et al.* Brazil’s unified health system: the first 30 years and prospects for the future. *The Lancet* **394**, 345–356 (2019).
- [39] Verity, R. *et al.* Estimates of the severity of coronavirus disease 2019: A model-based analysis. *The Lancet Infectious Diseases* **20**, 669–677 (2020).
- [40] Heroy, S. Metropolitan-scale COVID-19 outbreaks: How similar are they? *arXiv:2004.01248* (2020).
- [41] Brasil.io – Boletins informativos e casos do coronavírus por município por dia. Available: <https://brasil.io/dataset/covid19/caso/>. Accessed: 27 May 2020.
- [42] Brazil’s Public healthcare System (SUS), Department of Data Processing (DATASUS). Available: <http://datasus.saude.gov.br>. Accessed: 27 May 2020.
- [43] Leitao, J. C., Miotto, J. M., Gerlach, M. & Altmann, E. G. Is this scaling nonlinear? *Royal Society Open Science* **3**, 150649 (2016).

City size and the spreading of COVID-19 in Brazil

Haroldo V. Ribeiro, Andre S. Sunahara, Jack Sutton, Matjaž Perc, and Quentin S. Hanley

PLOS ONE, 2020

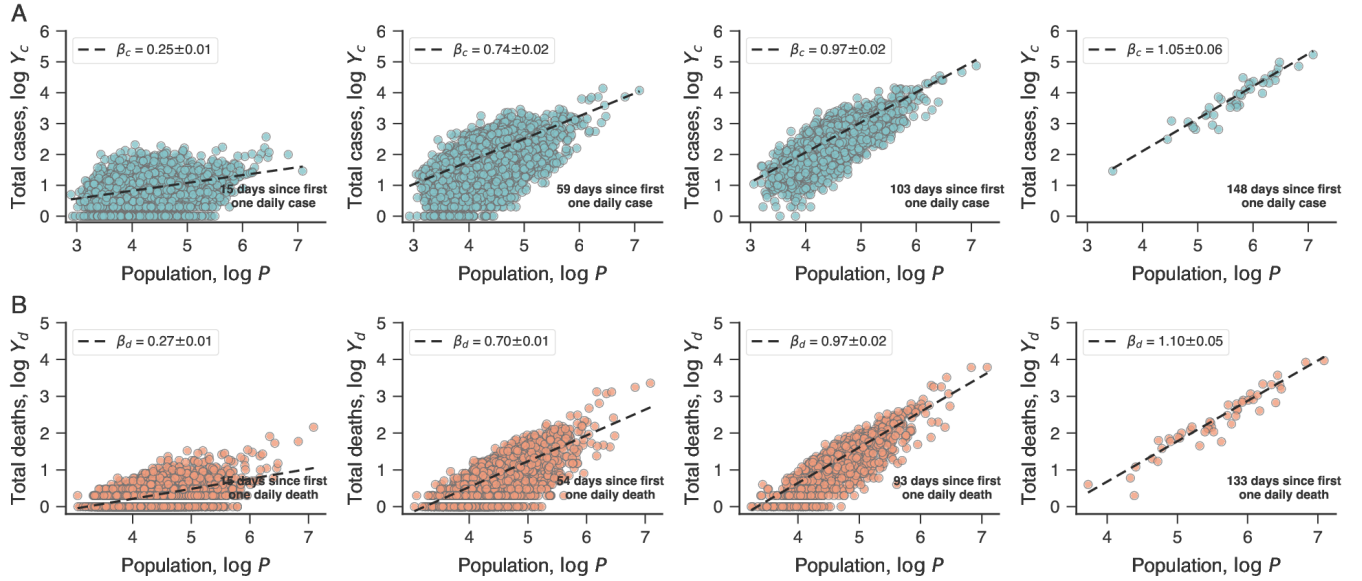


Figure 1. **Urban scaling relations of COVID-19 cases and deaths under different choices of values for the number of daily cases or daily deaths as reference points.** The same plots of Figure 1 in the main text but considering the first one daily case and first one daily death as reference points.

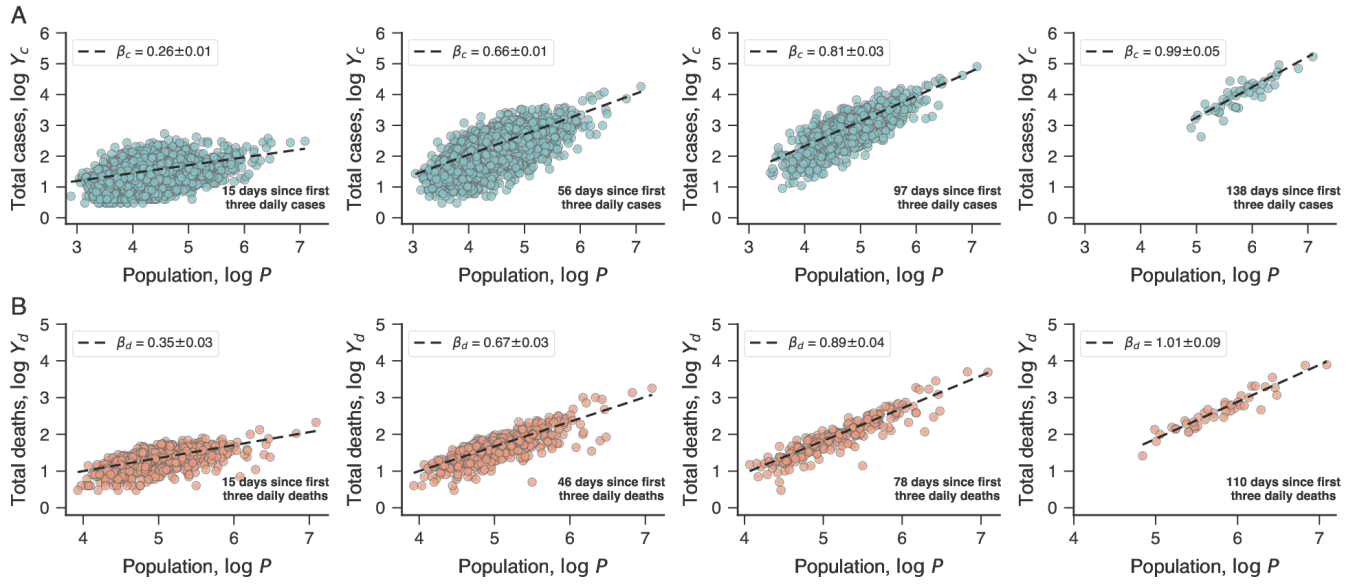


Figure 2. Urban scaling relations of COVID-19 cases and deaths under different choices of values for the number of daily cases or daily deaths as reference points. The same plots of Figure 1 in the main text but considering the first three daily cases and the first three daily deaths as reference points.

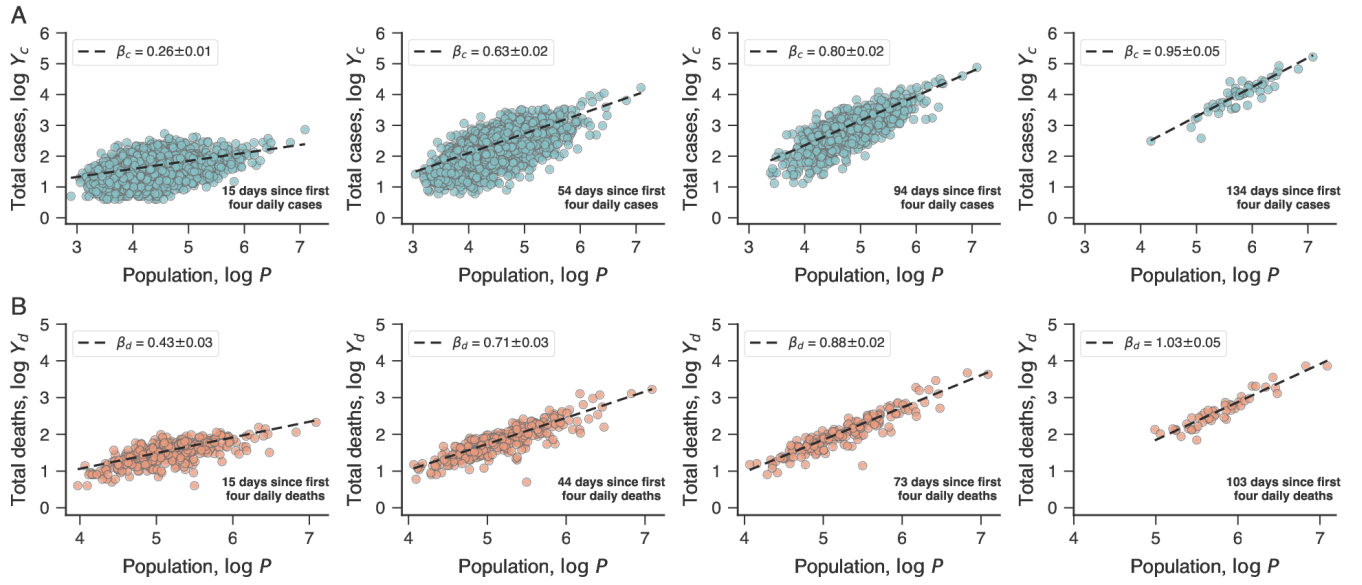


Figure 3. **Urban scaling relations of COVID-19 cases and deaths under different choices of values for the number of daily cases or daily deaths as reference points.** The same plots of Figure 1 in the main text but considering the first four daily cases and the first four daily deaths as reference points.

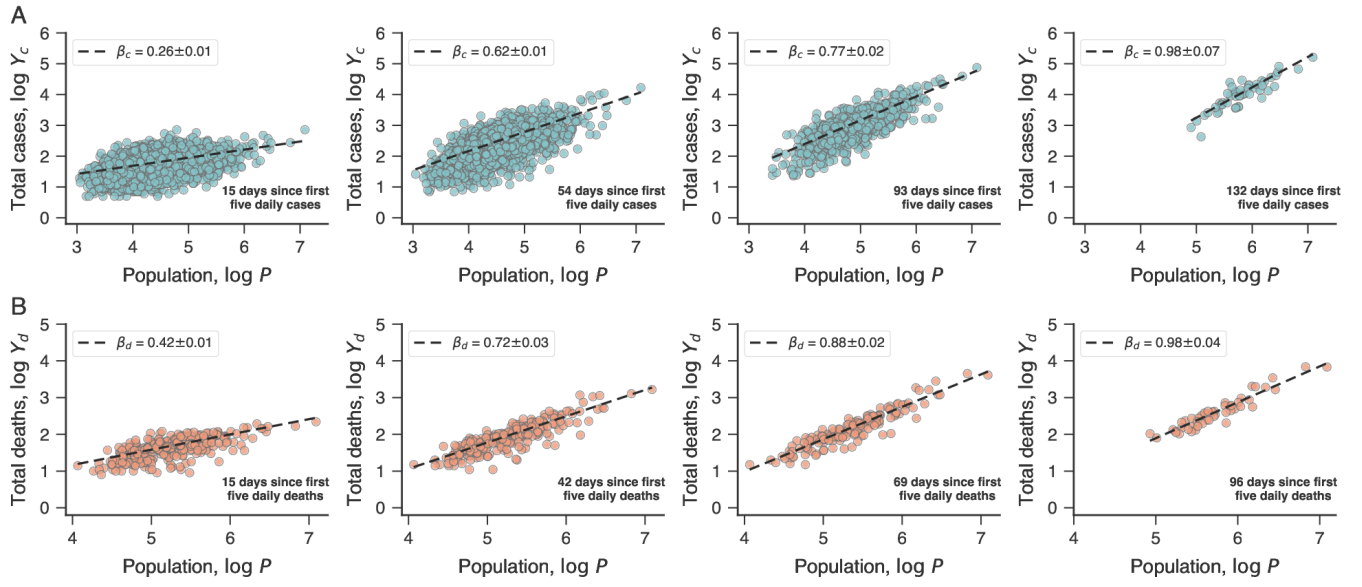


Figure 4. **Urban scaling relations of COVID-19 cases and deaths under different choices of values for the number of daily cases or daily deaths as reference points.** The same plots of Figure 1 in the main text but considering the first five daily cases and the first five daily deaths as reference points.

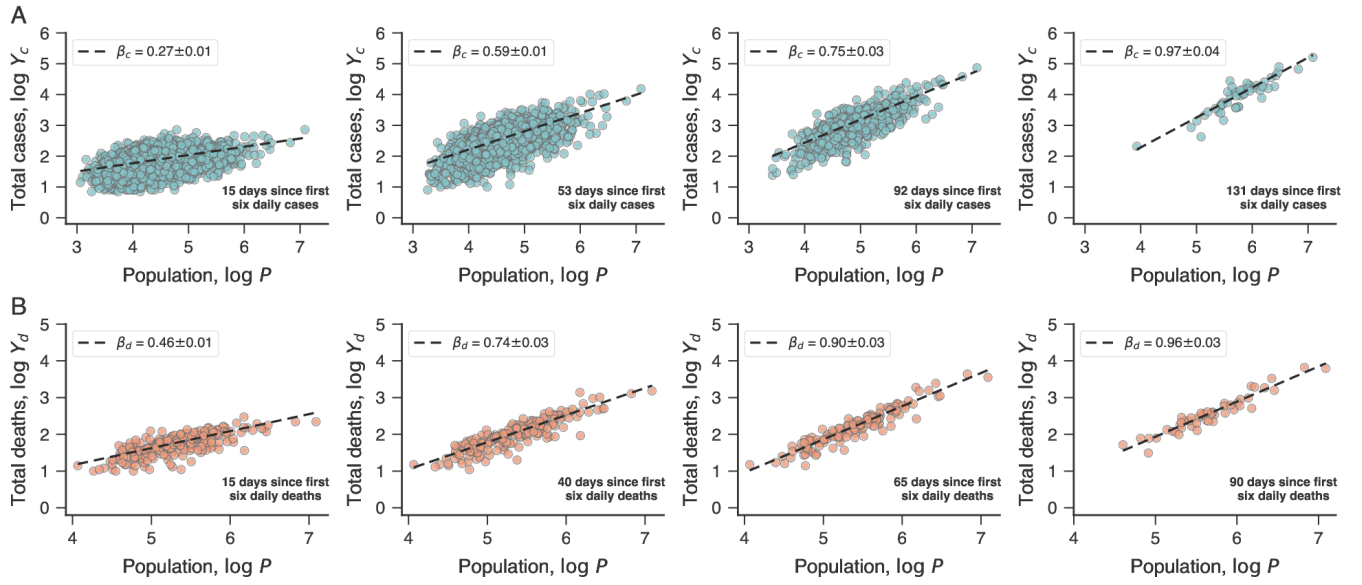


Figure 5. **Urban scaling relations of COVID-19 cases and deaths under different choices of values for the number of daily cases or daily deaths as reference points.** The same plots of Figure 1 in the main text but considering the first six daily cases and the first six daily deaths as reference points.

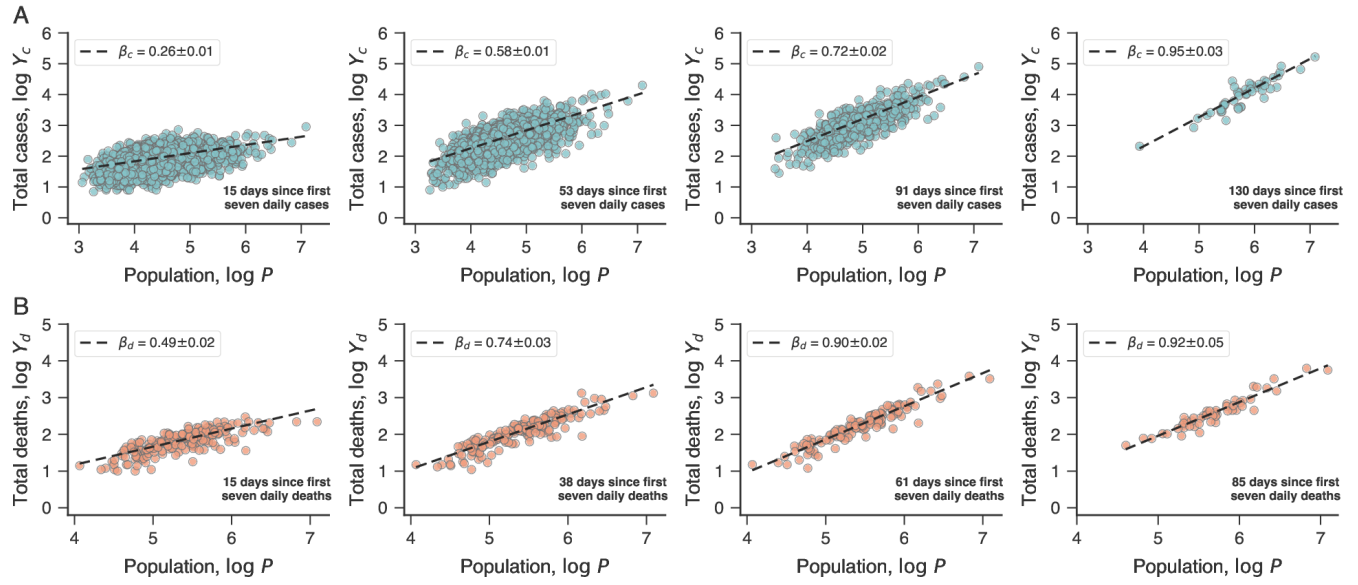


Figure 6. **Urban scaling relations of COVID-19 cases and deaths under different choices of values for the number of daily cases or daily deaths as reference points.** The same plots of Figure 1 in the main text but considering the first seven daily cases and the first seven daily deaths as reference points.

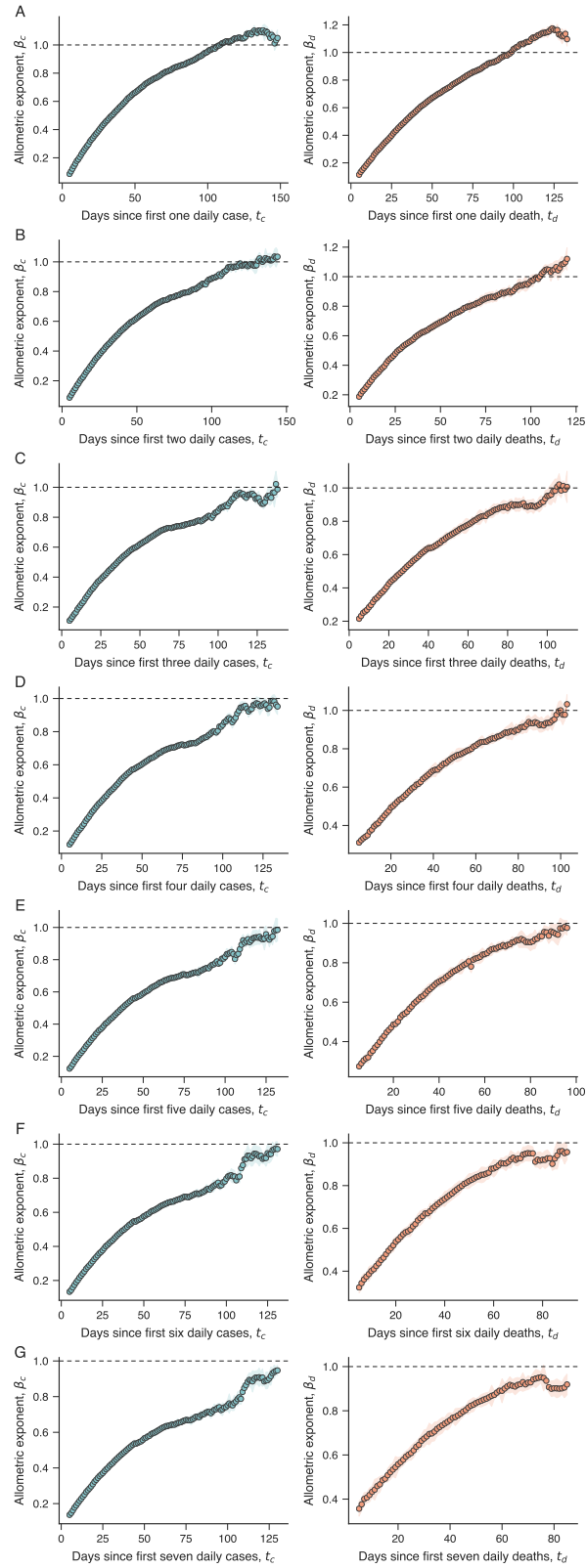


Figure 7. **Time dependence of the scaling exponents for COVID-19 cases and deaths under different choices of values for the number of daily cases or daily deaths as reference points.** Panels (A)-(G) show the dependence of the exponents β_c (left) and β_d (right) on t_c and t_d when considering the first 1-7 daily cases and the first 1-7 daily deaths as reference points. The shaded regions stand for standard errors, and the horizontal dashed lines represent $\beta_c = \beta_d = 1$. We note that the behavior observed for large numbers of the reference points appear to follow the behavior of small ones in the long-term course of the pandemic.

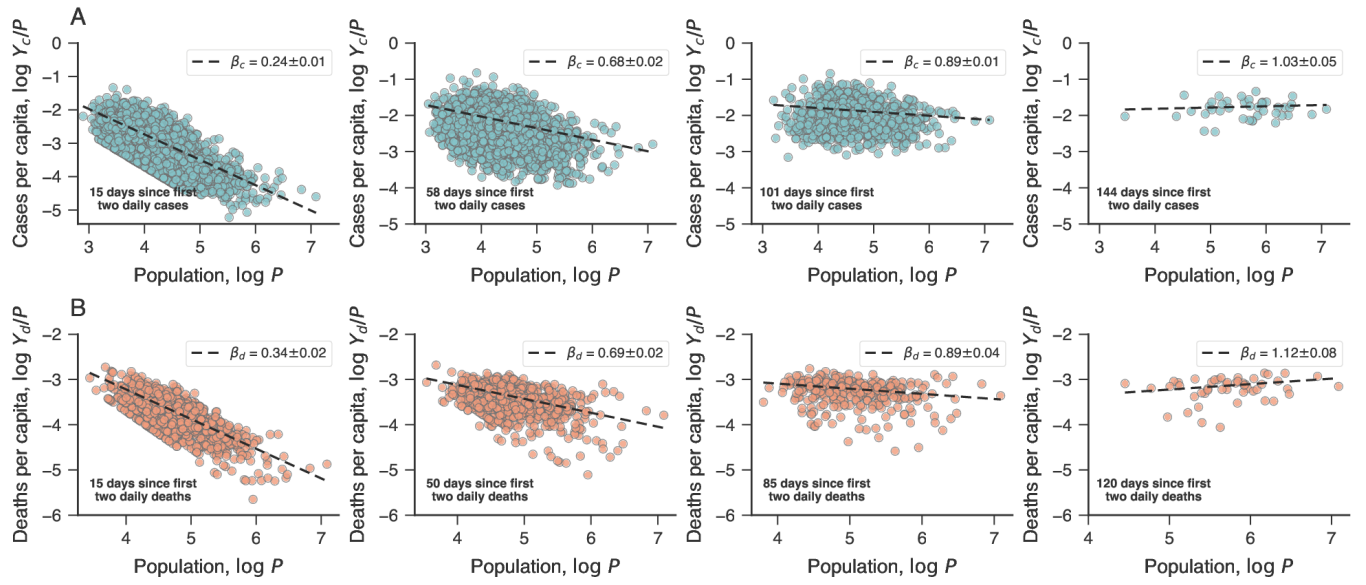


Figure 8. **Urban scaling relations of COVID-19 cases and deaths *per capita*.** (A) Relationship between the total of confirmed cases *per capita* of COVID-19 (Y_c/P) and city population (P) on logarithmic scale. (B) Relationship between the total of deaths *per capita* caused by COVID-19 (Y_d) and population (P) of Brazilian cities (on logarithmic scale). Panels show scaling relations on a particular day after the first two daily cases or the first two daily deaths. The dashed lines are the scaling relations with exponents indicated in each plot ($\beta_c - 1$ for cases *per capita* and $\beta_d - 1$ for deaths *per capita*).

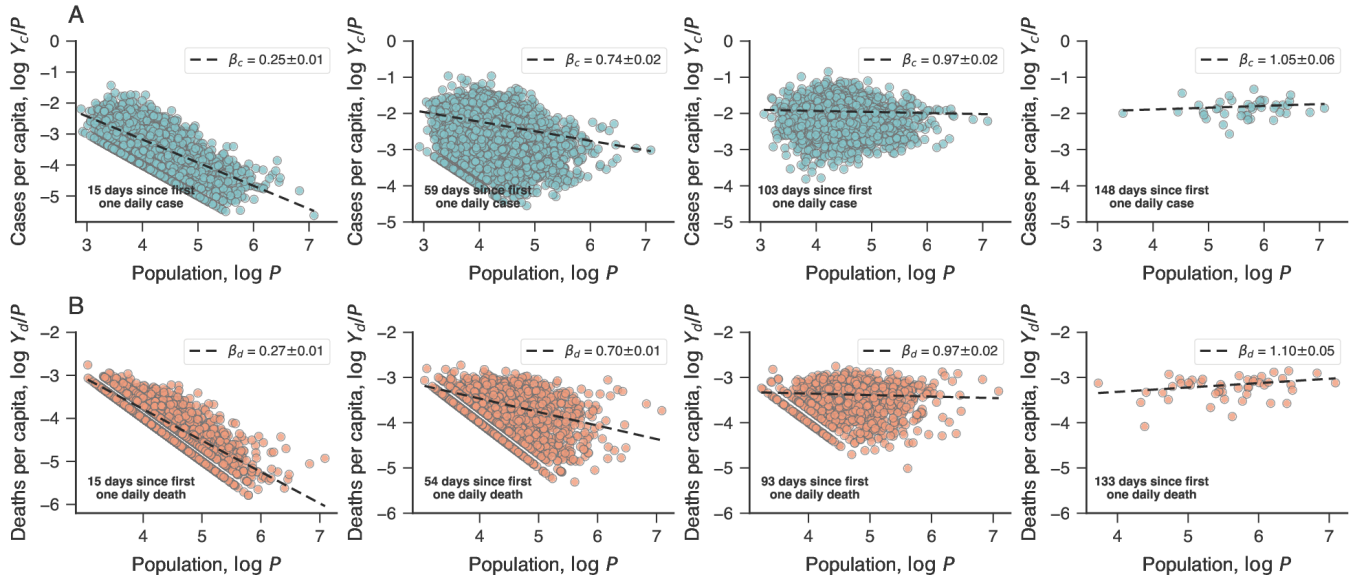


Figure 9. **Urban scaling relations of COVID-19 cases and deaths *per capita*.** The same as Figure 8 in this Appendix, but considering the first one daily case and the first one daily death as reference points.

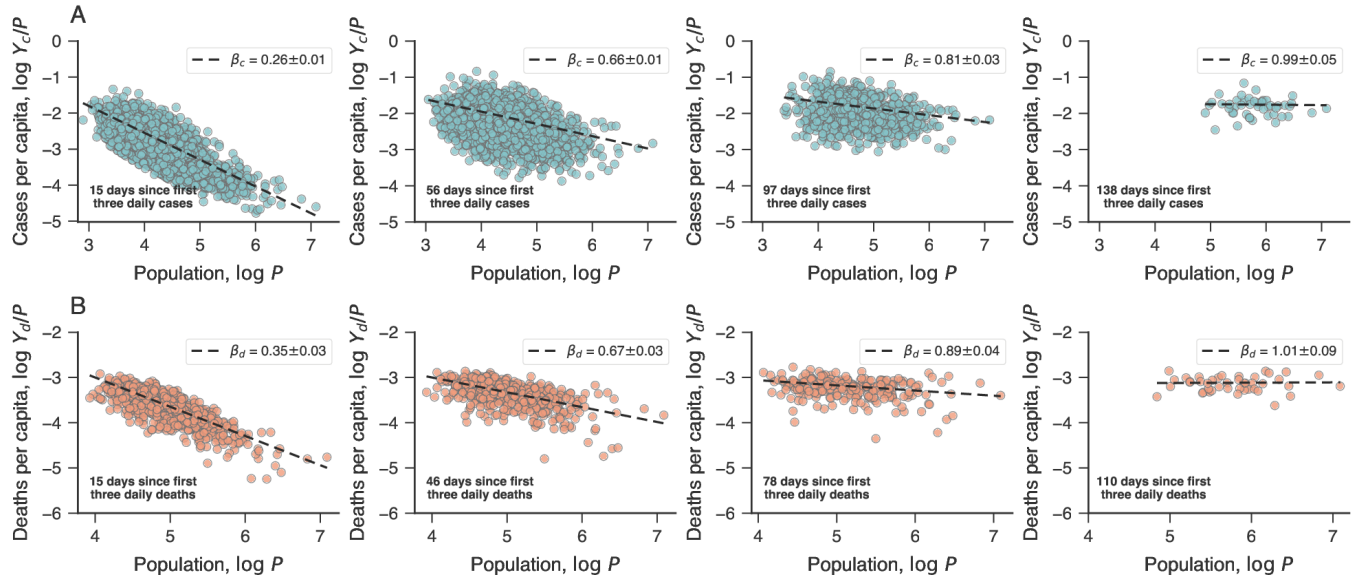


Figure 10. **Urban scaling relations of COVID-19 cases and deaths *per capita*.** The same as Figure 8 in this Appendix, but considering the first three daily cases and the first three daily deaths as reference points.

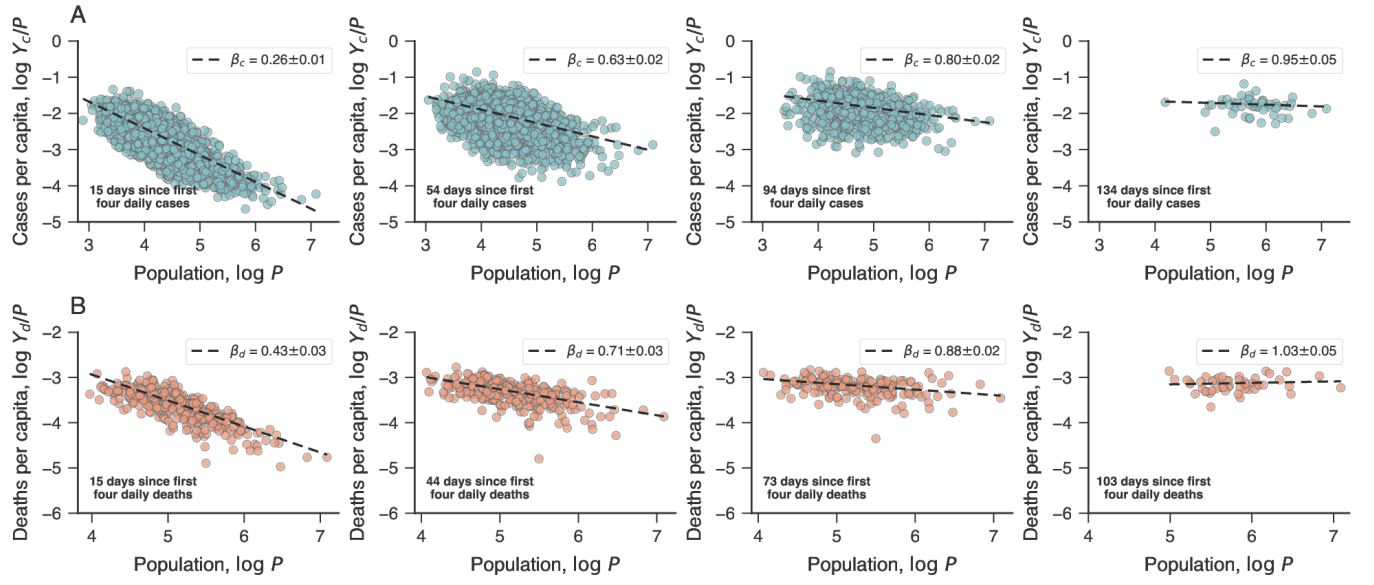


Figure 11. **Urban scaling relations of COVID-19 cases and deaths *per capita*.** The same as Figure 8 in this Appendix, but considering the first four daily cases and the first four daily deaths as reference points.

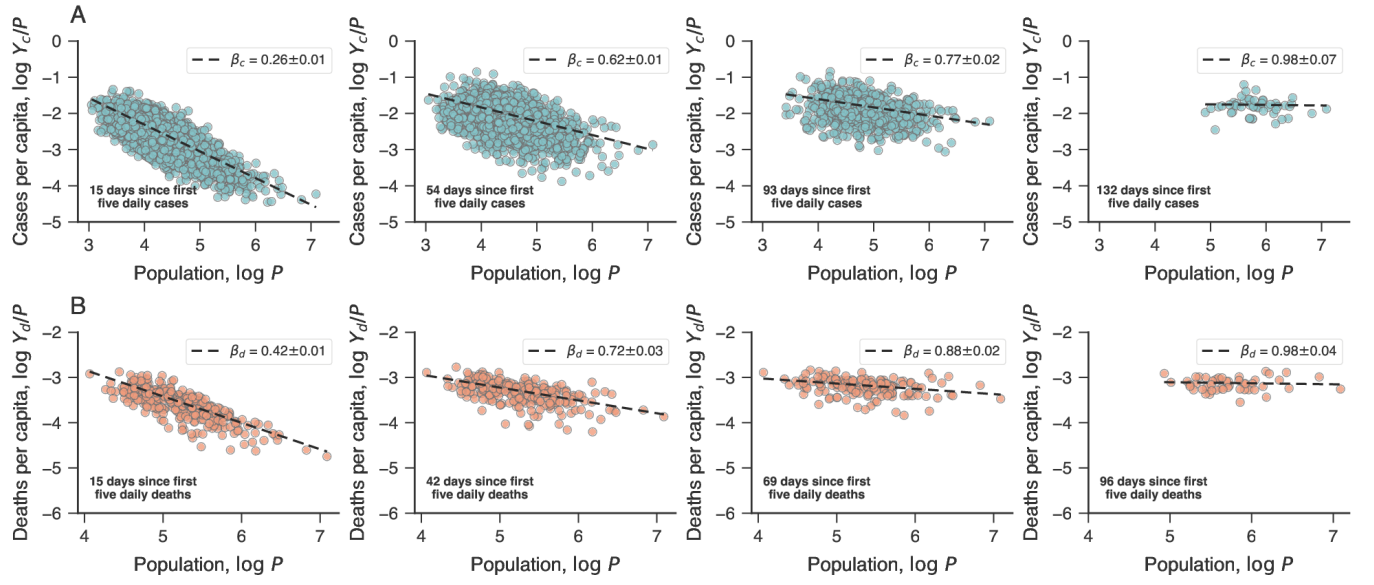


Figure 12. **Urban scaling relations of COVID-19 cases and deaths *per capita*.** The same as Figure 8 in this Appendix, but considering the first five cases and the first five daily deaths as reference points.

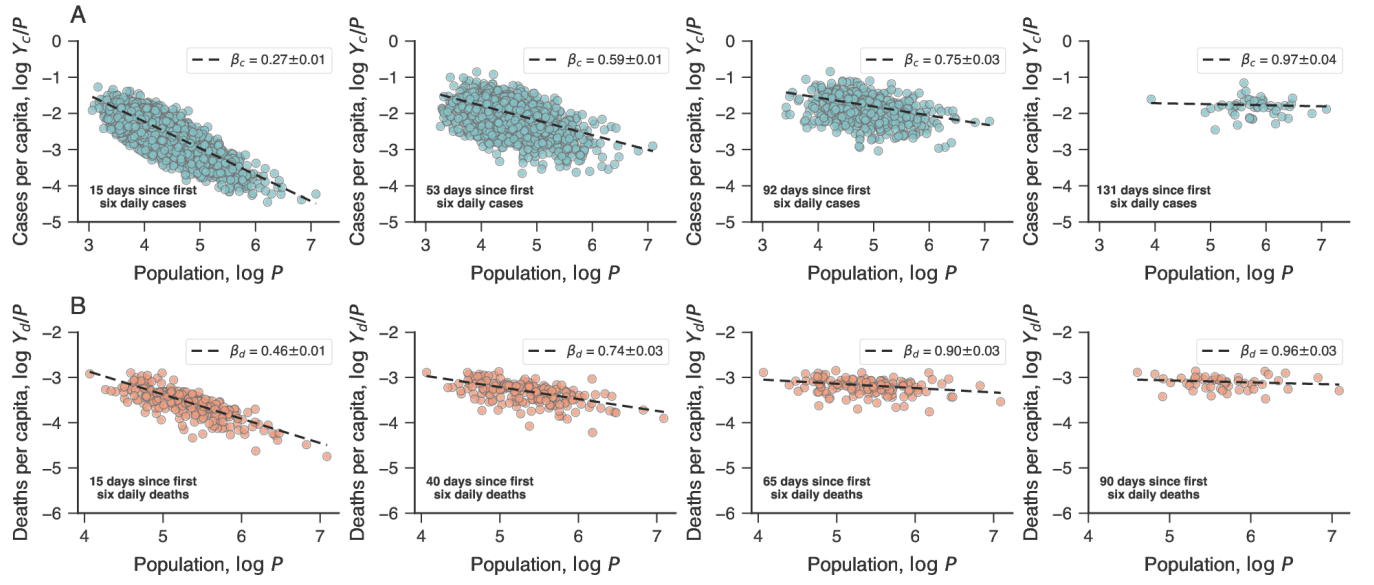


Figure 13. **Urban scaling relations of COVID-19 cases and deaths *per capita*.** The same as Figure 8 in this Appendix, but considering the first six daily cases and the first six daily deaths as reference points.

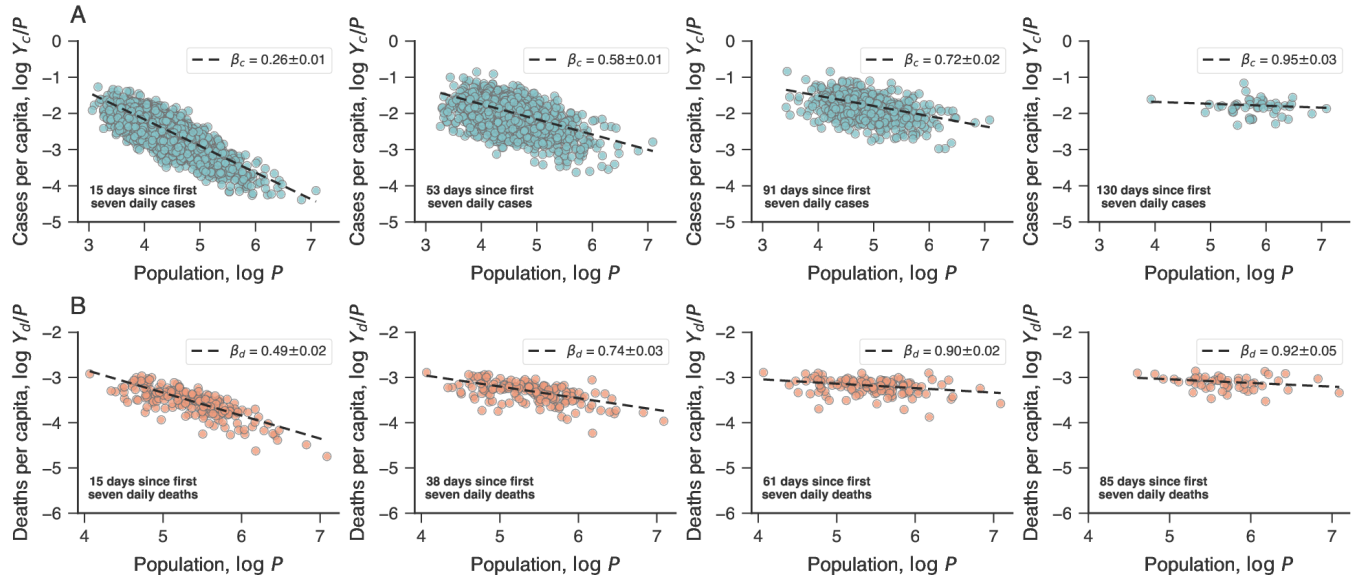


Figure 14. **Urban scaling relations of COVID-19 cases and deaths *per capita*.** The same as Figure 8 in this Appendix, but considering the first seven daily cases and the first seven daily deaths as reference points.

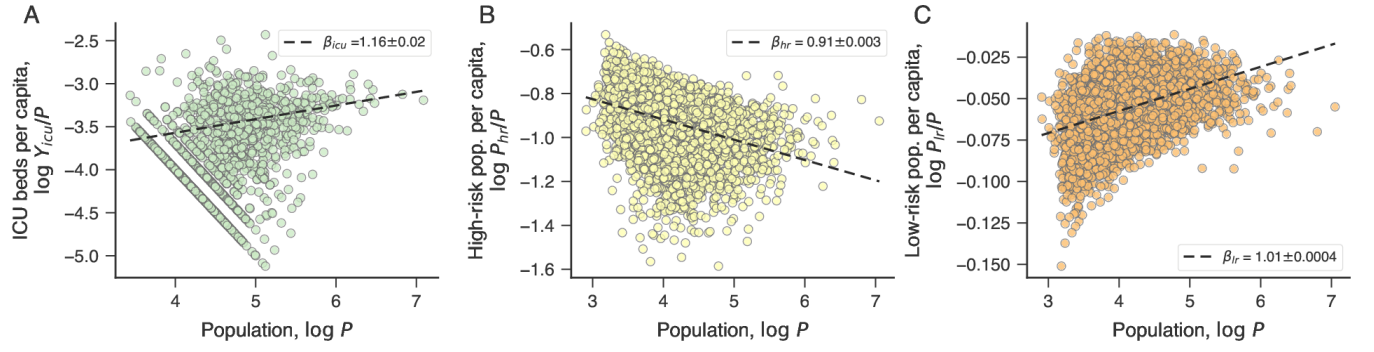


Figure 15. **Urban scaling of ICU beds, high-risk and low-risk populations *per capita*.** (A) Relationship between the number of ICU beds *per capita* (Y_{icu}/P) and the city population (P) on logarithmic scale. (B) Relationship between the high-risk population *per capita* (P_{hr}/P) and the city population (P) on logarithmic scale. (C) Relationship between low-risk population *per capita* (P_{lr}/P) and the city population (P) on logarithmic scale. In all panels, the dashed lines are the scaling relations with exponents indicated in each plot ($\beta_{icu} - 1$ for ICU beds *per capita*, $\beta_{hr} - 1$ for high-risk population *per capita*, and $\beta_{lr} - 1$ for low-risk population *per capita*).

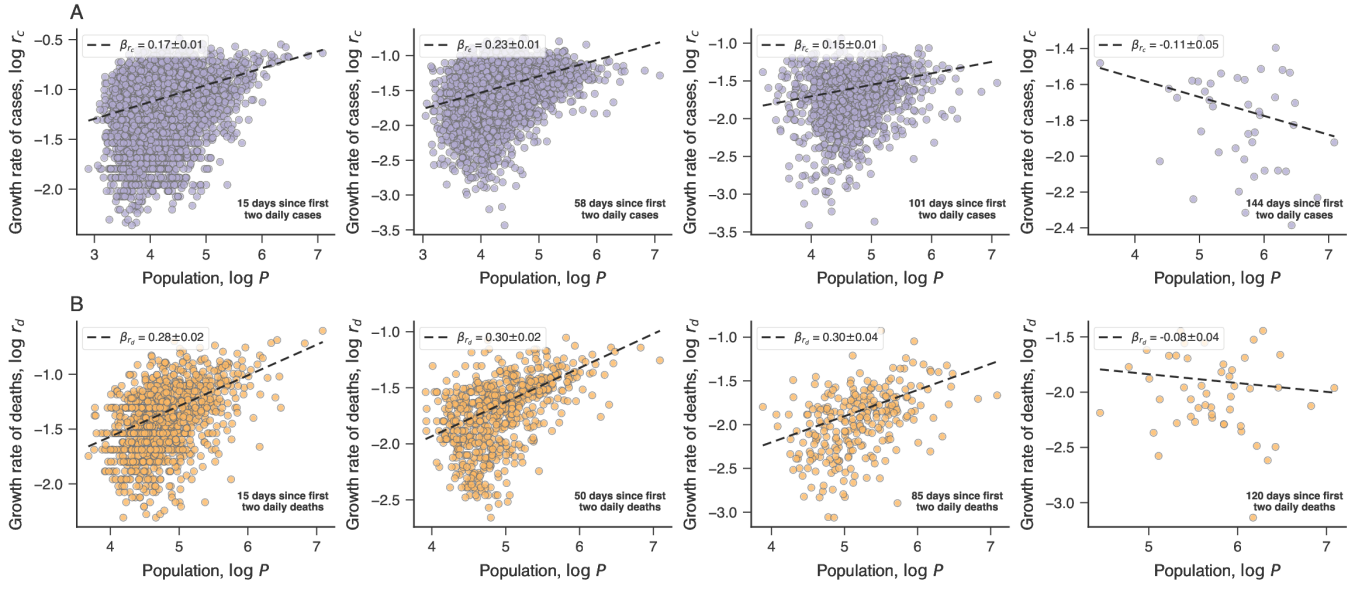


Figure 16. **Urban scaling relations of growth rates of COVID-19 cases and deaths.** (A) Relationship between the growth rate of cases (r_c) and the city population (P) on logarithmic scale. Panels show scaling relations for values of r_c estimated after a given number of days since the first two daily cases (four evenly spaced values of t_c between 15 days and the largest value yielding at least 50 cities, as indicated within panels). (B) Relationship between the growth rate of deaths (r_d) and the city population (P) on logarithmic scale. Panels show scaling relations for values of r_d estimated after a given number of days since the first two daily deaths (four evenly spaced values of t_d between 15 days and the largest value yielding at least 50 cities, as indicated within panels). The markers in (A) and (B) represent cities, and the dashed lines are the adjusted scaling relations with best-fitting exponents indicated in each plot (β_{r_c} for the growth rate of cases and β_{r_d} for the growth rate of deaths). All rates were estimated using $\tau = 14$ as defined in Eq. (5) of the main text.

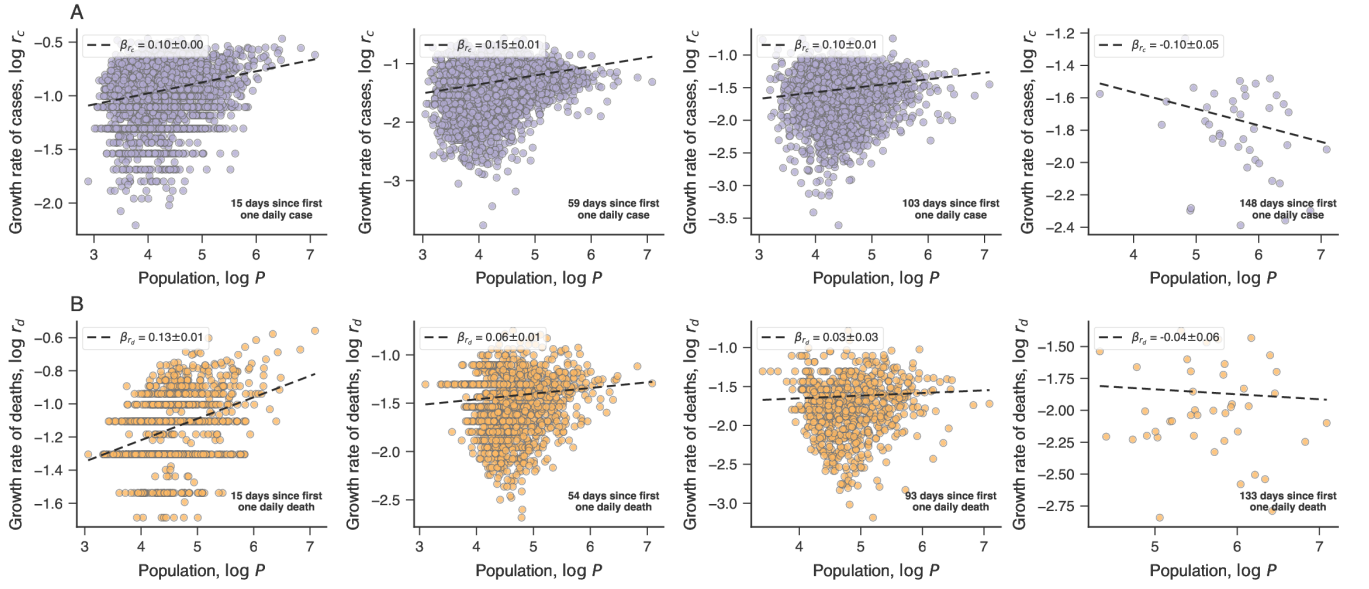


Figure 17. **Urban scaling relations of growth rates of COVID-19 cases and deaths.** The same as Figure 16 in this Appendix, but considering the first one daily case and first one daily death as reference points.

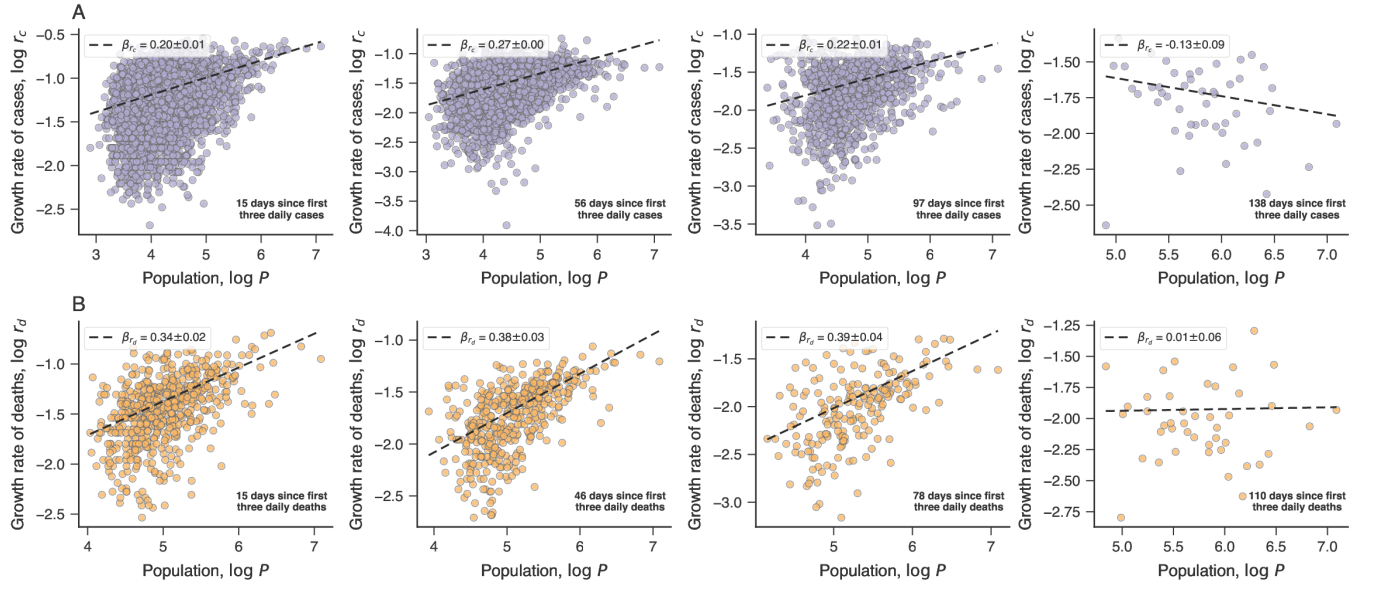


Figure 18. **Urban scaling relations of growth rates of COVID-19 cases and deaths.** The same as Figure 16 in this Appendix, but considering three daily cases and three daily deaths as reference points.

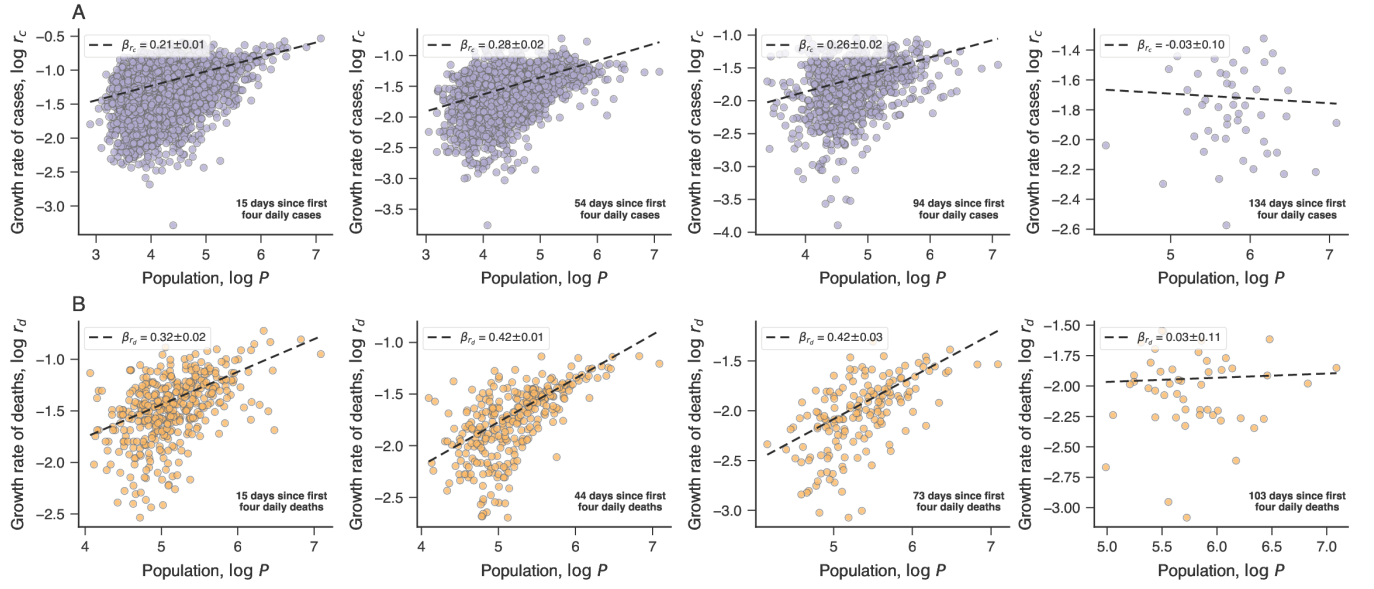


Figure 19. **Urban scaling relations of growth rates of COVID-19 cases and deaths.** The same as Figure 16 in this Appendix, but considering four daily cases and four daily deaths as reference points.

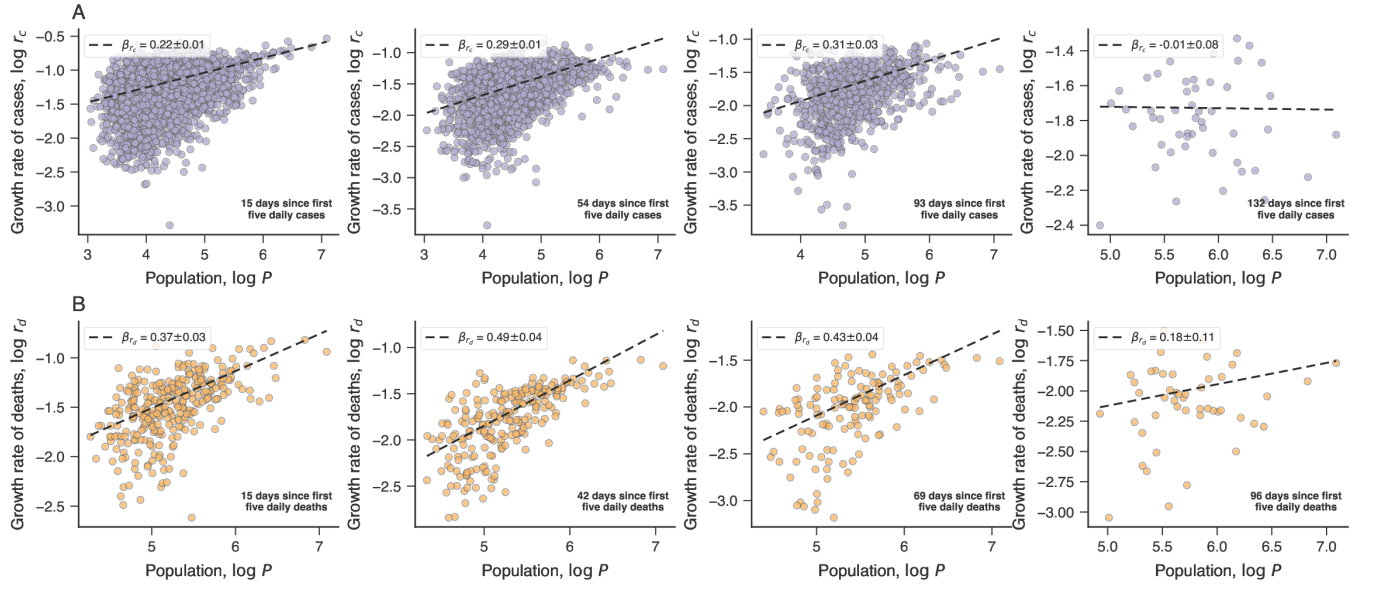


Figure 20. **Urban scaling relations of growth rates of COVID-19 cases and deaths.** The same as Figure 16 in this Appendix, but considering five daily cases and five daily deaths as reference points.

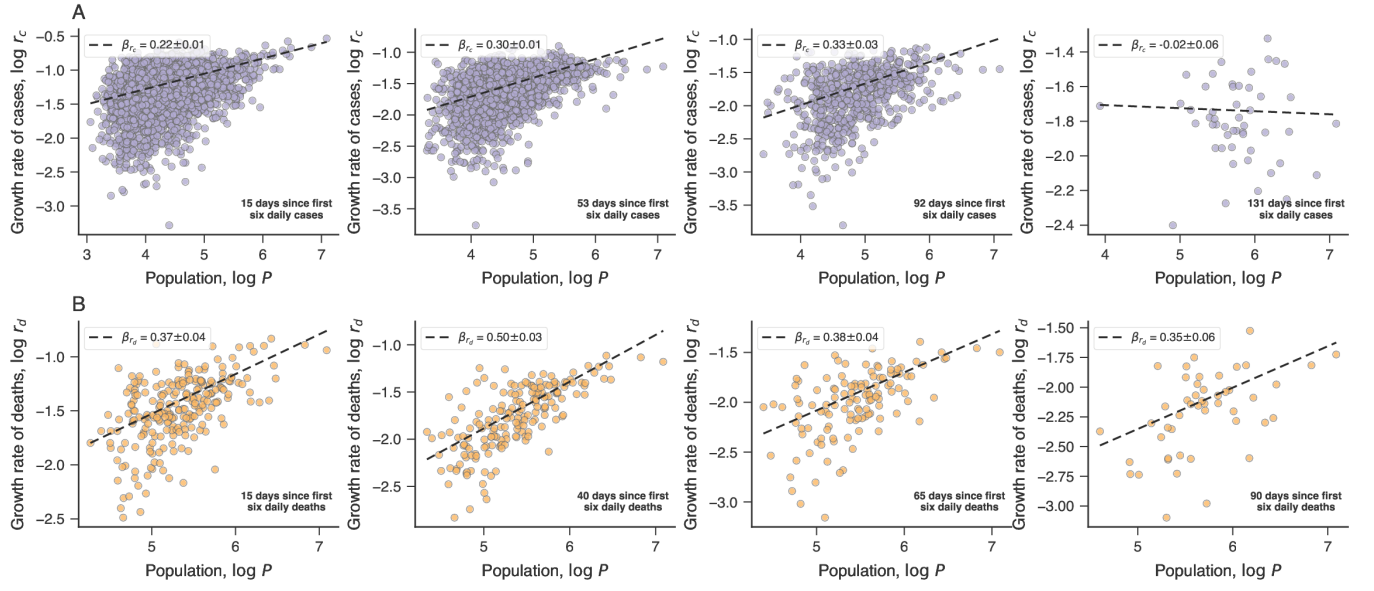


Figure 21. **Urban scaling relations of growth rates of COVID-19 cases and deaths.** The same as Figure 16 in this Appendix, but considering six daily cases and six daily deaths as reference points.

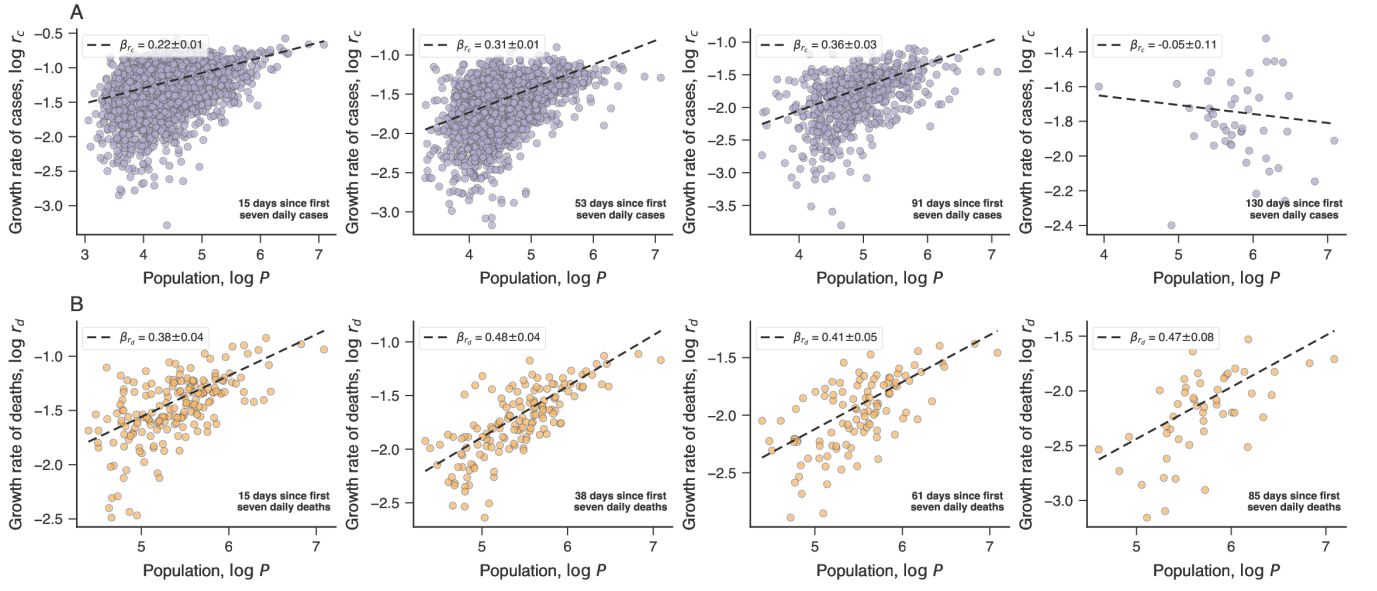


Figure 22. **Urban scaling relations of growth rates of COVID-19 cases and deaths.** The same as Figure 16 in this Appendix, but considering seven daily cases and seven daily deaths as reference points.

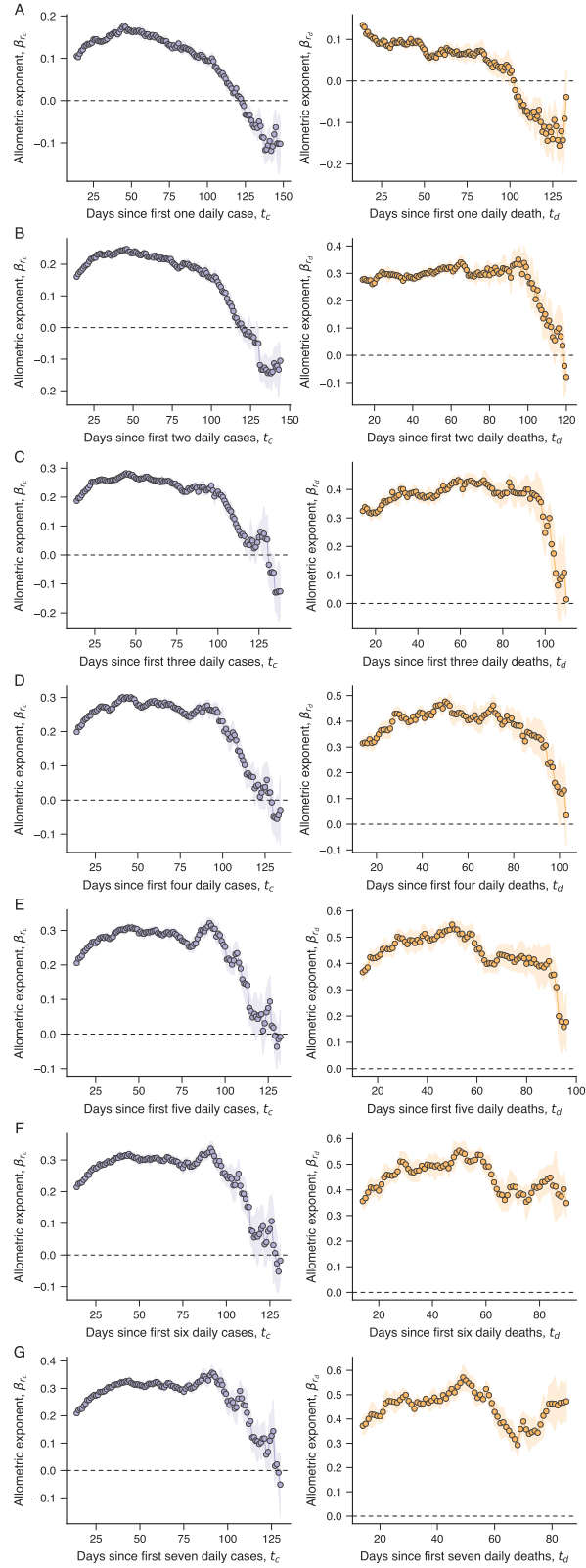


Figure 23. **Time dependence of the scaling exponents for growth rates of cases and deaths under different choices for the number of daily cases or daily deaths as reference points.** Panels (A)-(G) show the dependence of the exponents β_{r_c} and β_{r_d} on t_c and t_d when considering the first 1-7 daily cases and the first 1-7 daily deaths as reference points. The shaded regions stand for standard errors, and the horizontal dashed lines represent $\beta_{r_c} = \beta_{r_d} = 0$. We notice that behavior observed for large numbers of the reference points appear to follow the behavior of small ones in the long-term course of the pandemic.

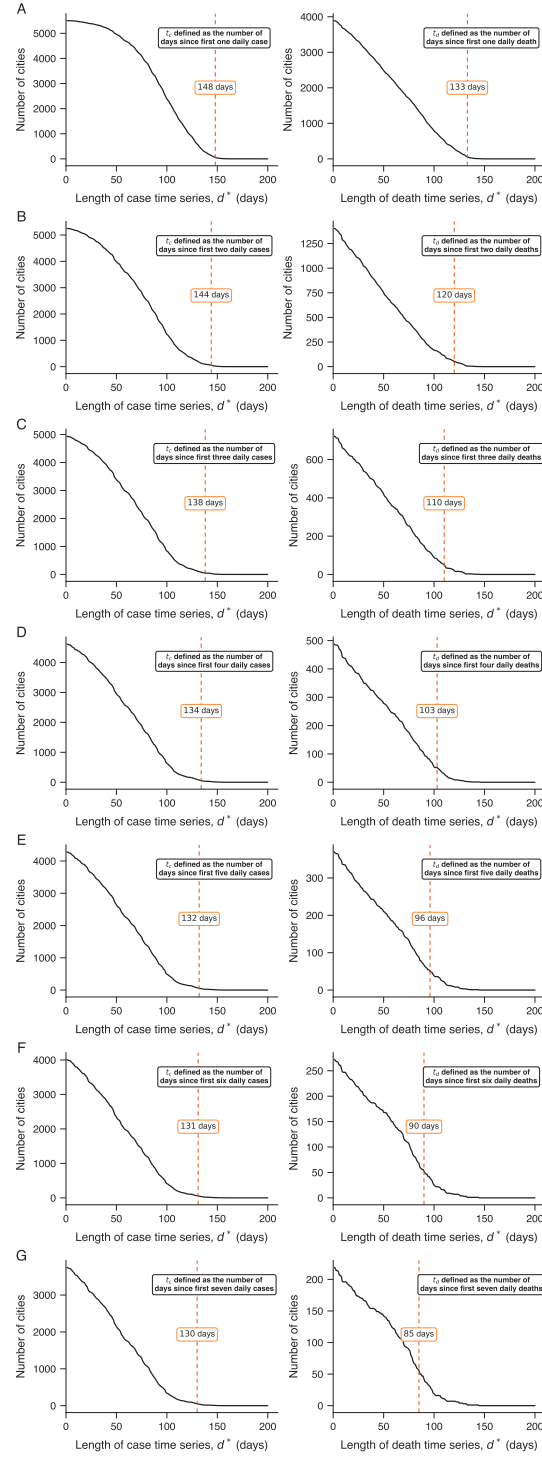


Figure 24. **Number of cities with time series longer than a particular number of days.** Left panels show the number of cities reporting cases of COVID-19 with time series larger than d^* days. The vertical dashed lines indicate that there are 50 cities with confirmed cases time series longer than the particular of number of days indicated within the plots. Right panels show the number of cities reporting deaths caused by COVID-19 with time series longer than d^* days. The vertical dashed lines indicate that there are 50 cities with deaths time series longer than the particular of number of days indicated within the plots. We have used these thresholds to ensure that our scaling relations are estimated from samples sizes having at least 50 cities. Panels (A)-(G) show the results when considering the first 1-7 daily cases and the first 1-7 daily deaths as reference points.

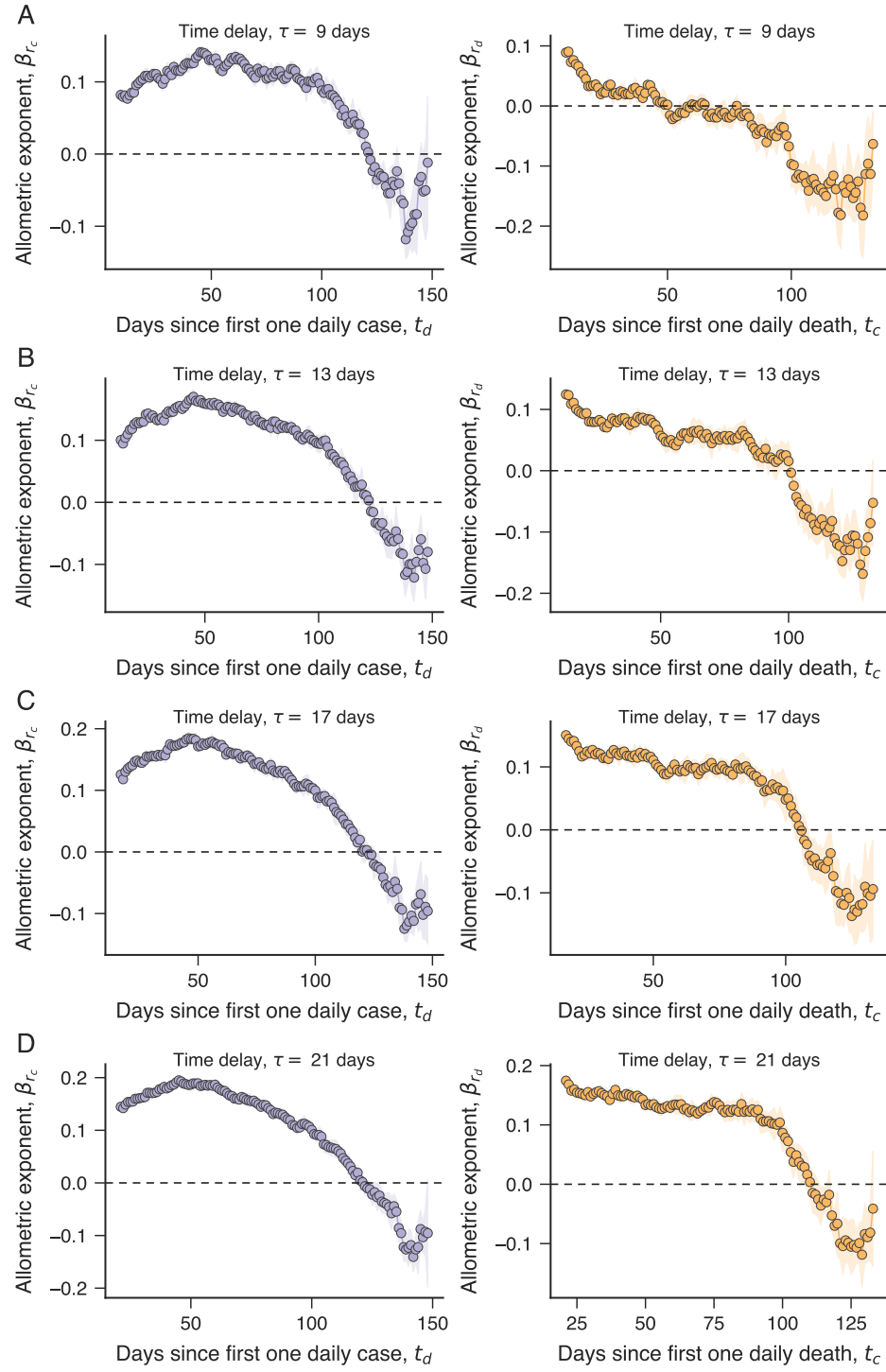


Figure 25. **Variations in the scaling exponents for the growth rates of cases and deaths under different values of time delay τ .** Panels (A)-(D) show the dependence of the exponent β_{r_c} (left panels) and β_{r_d} (right panels) on the number of days since the first one daily case (t_c) or death (t_d) for different values of τ .

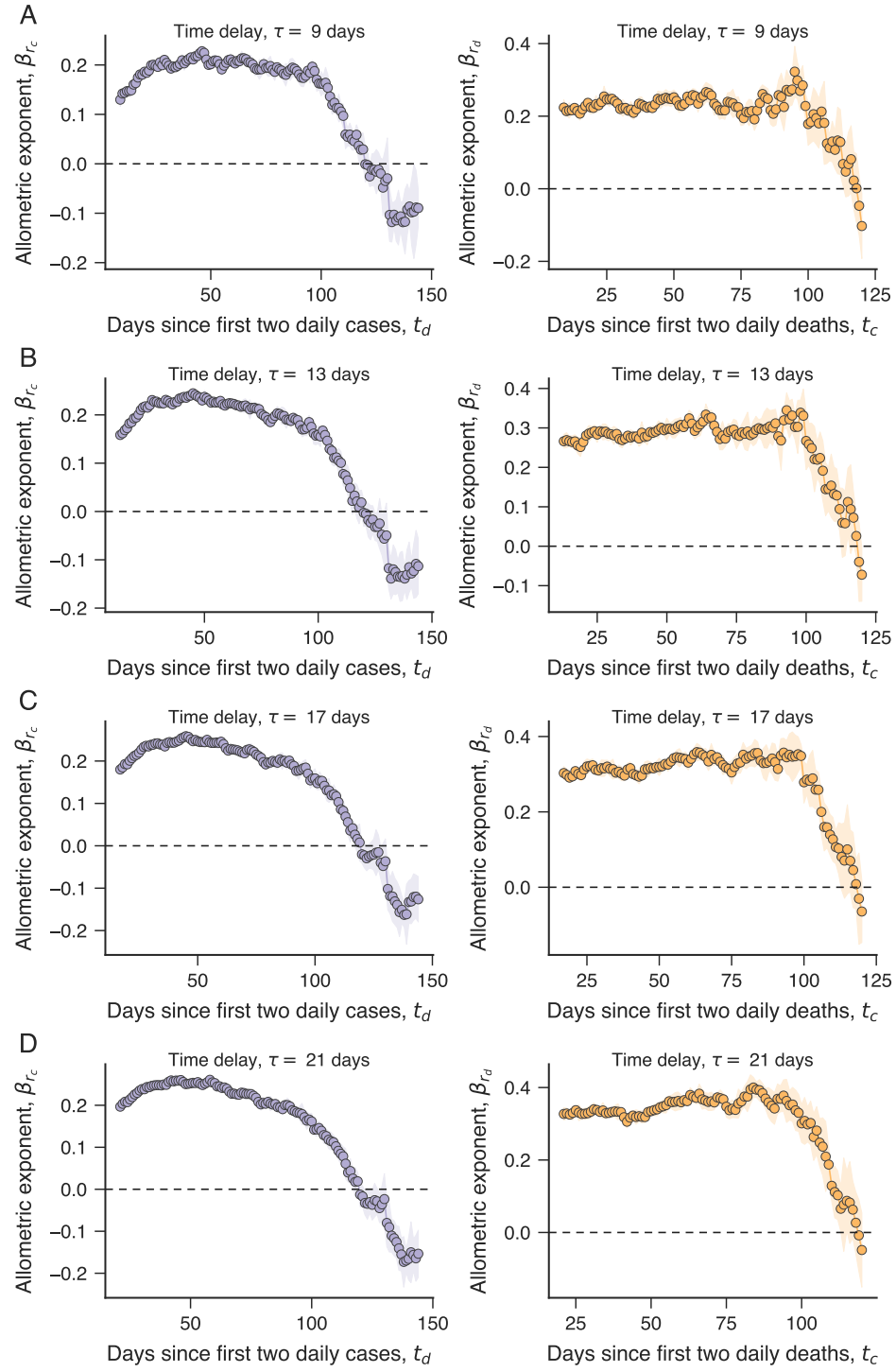


Figure 26. **Variations in the scaling exponents for the growth rates of cases and deaths under different values of time delay τ .** Panels (A)-(D) show the dependence of the exponent β_{r_c} (left panels) and β_{r_d} (right panels) on the number of days since the first two daily cases (t_c) or deaths (t_d) for different values of τ .

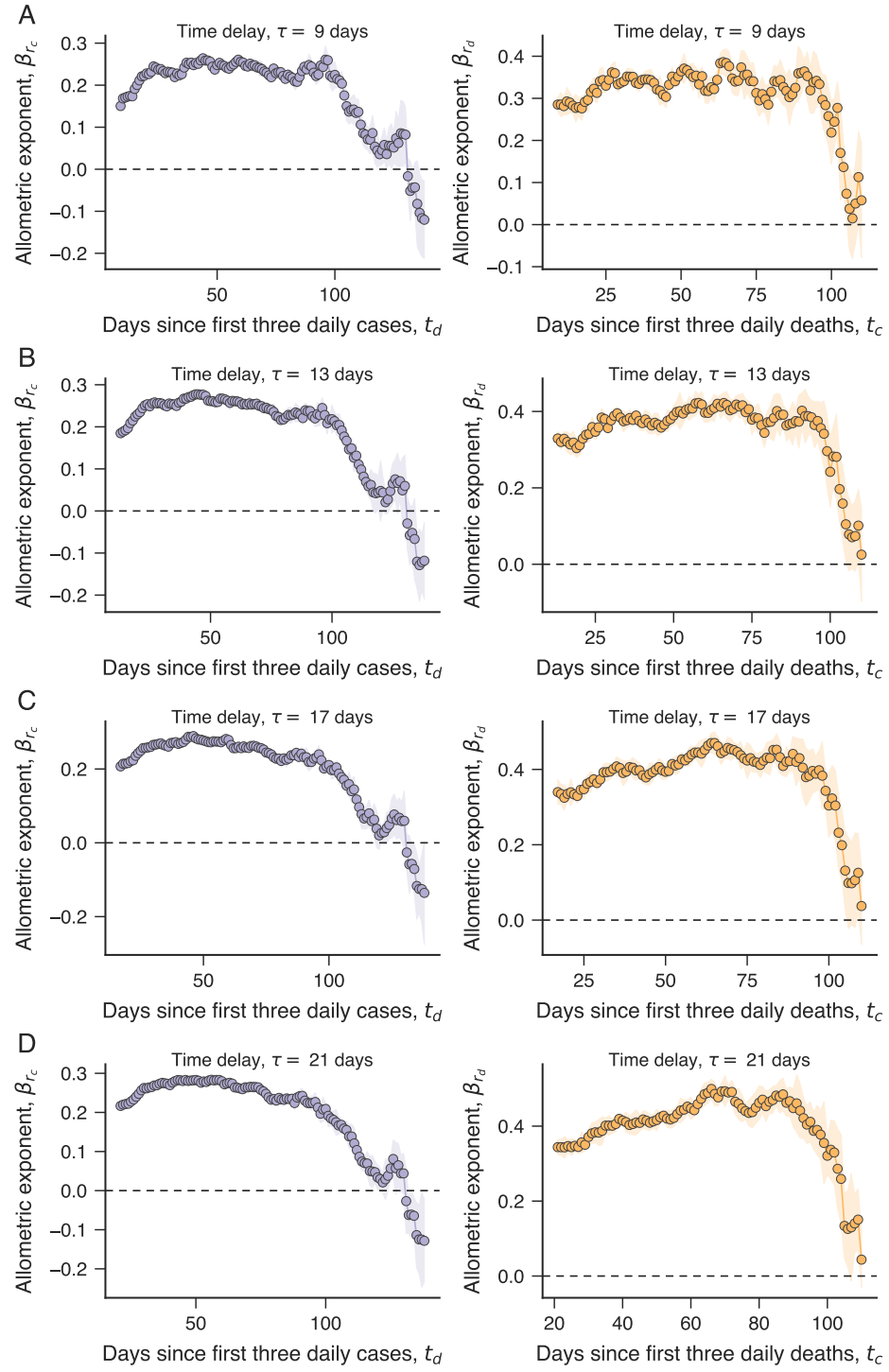


Figure 27. **Variations in the scaling exponents for the growth rates of cases and deaths under different values of time delay τ .** Panels (A)-(D) show the dependence of the exponent β_{r_c} (left panels) and β_{r_d} (right panels) on the number of days since the first three daily cases (t_c) or deaths (t_d) for different values of τ .

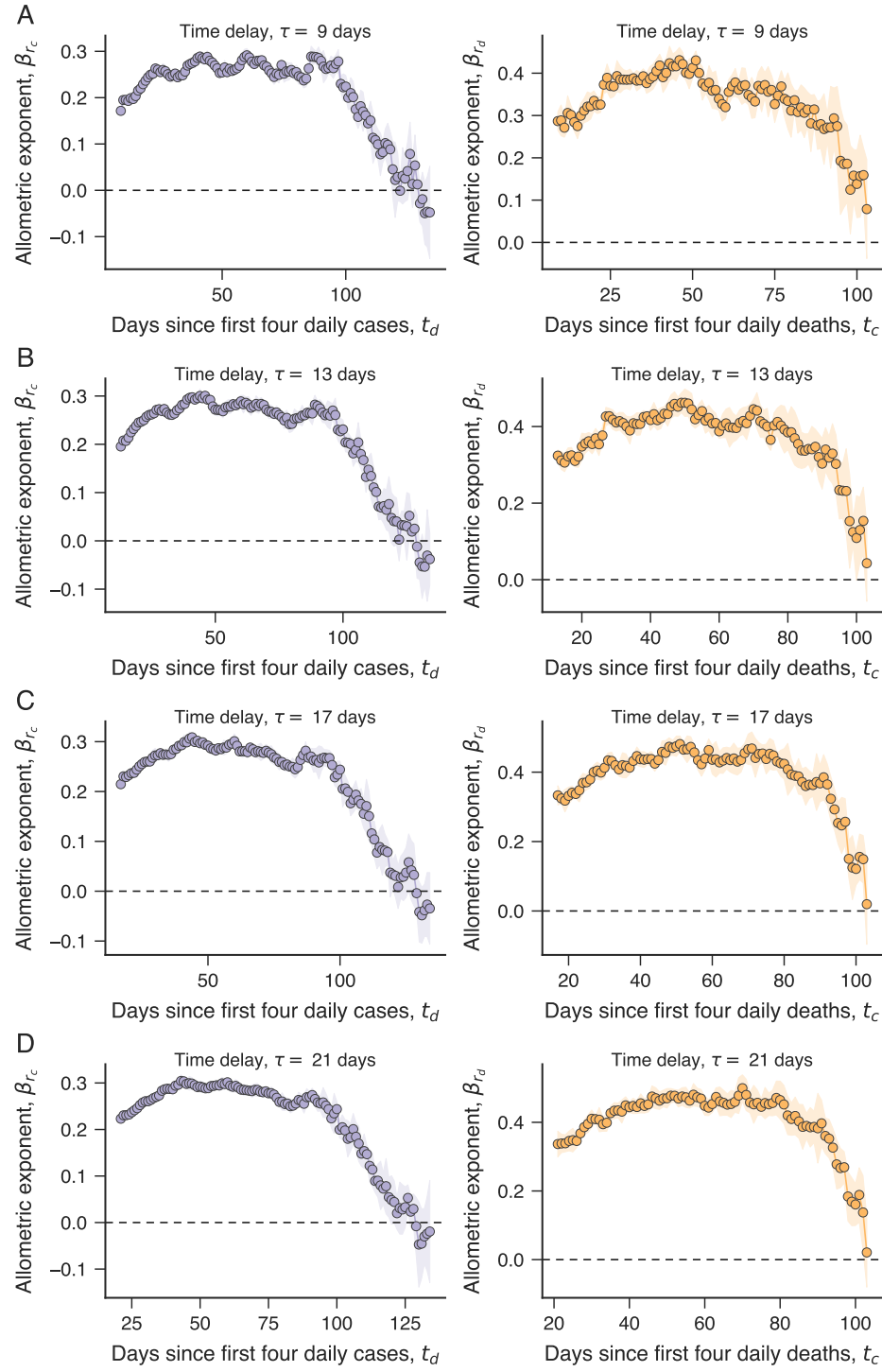


Figure 28. **Variations in the scaling exponents for the growth rates of cases and deaths under different values of time delay τ .** Panels (A)-(D) show the dependence of the exponent β_{r_c} (left panels) and β_{r_d} (right panels) on the number of days since the first four daily cases (t_c) or deaths (t_d) for different values of τ .

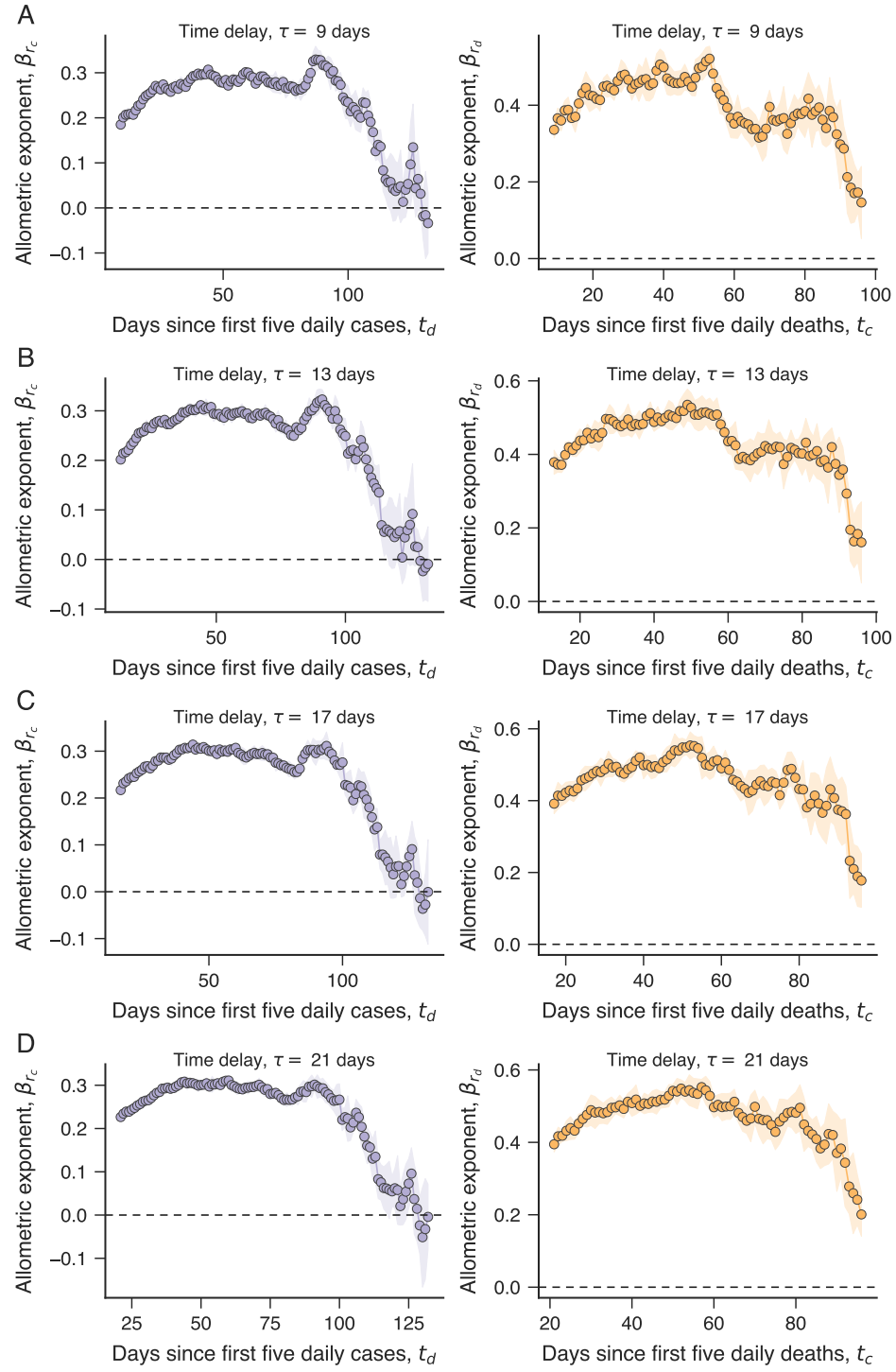


Figure 29. **Variations in the scaling exponents for the growth rates of cases and deaths under different values of time delay τ .** Panels (A)-(D) show the dependence of the exponent β_{r_c} (left panels) and β_{r_d} (right panels) on the number of days since the first five daily cases (t_c) or deaths (t_d) for different values of τ .

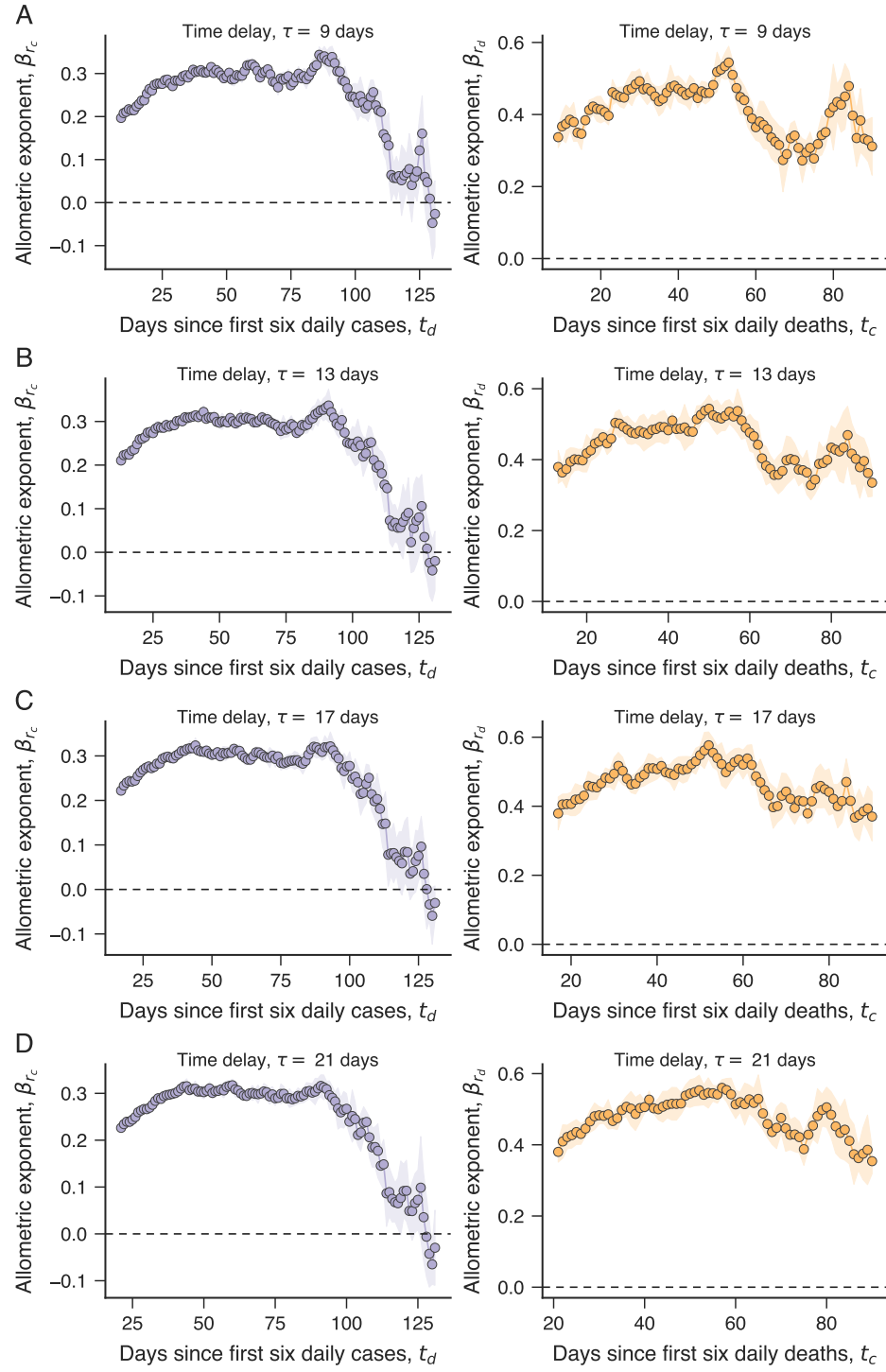


Figure 30. **Variations in the scaling exponents for the growth rates of cases and deaths under different values of time delay τ .** Panels (A)-(D) show the dependence of the exponent β_{r_c} (left panels) and β_{r_d} (right panels) on the number of days since the first six daily cases (t_c) or deaths (t_d) for different values of τ .

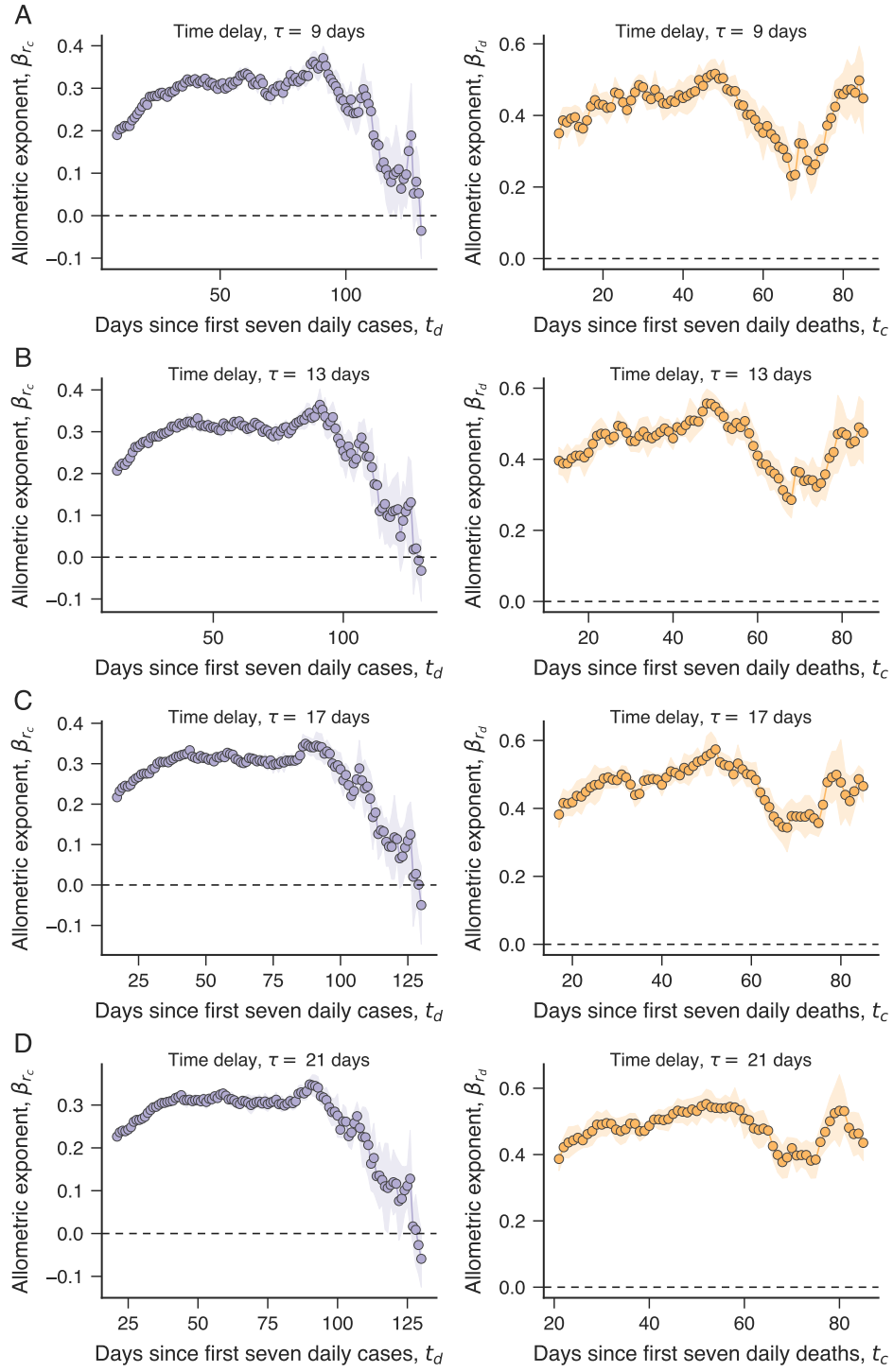


Figure 31. **Variations in the scaling exponents for the growth rates of cases and deaths under different values of time delay τ .** Panels (A)-(D) show the dependence of the exponent β_{r_c} (left panels) and β_{r_d} (right panels) on the number of days since the first seven daily cases (t_c) or deaths (t_d) for different values of τ .

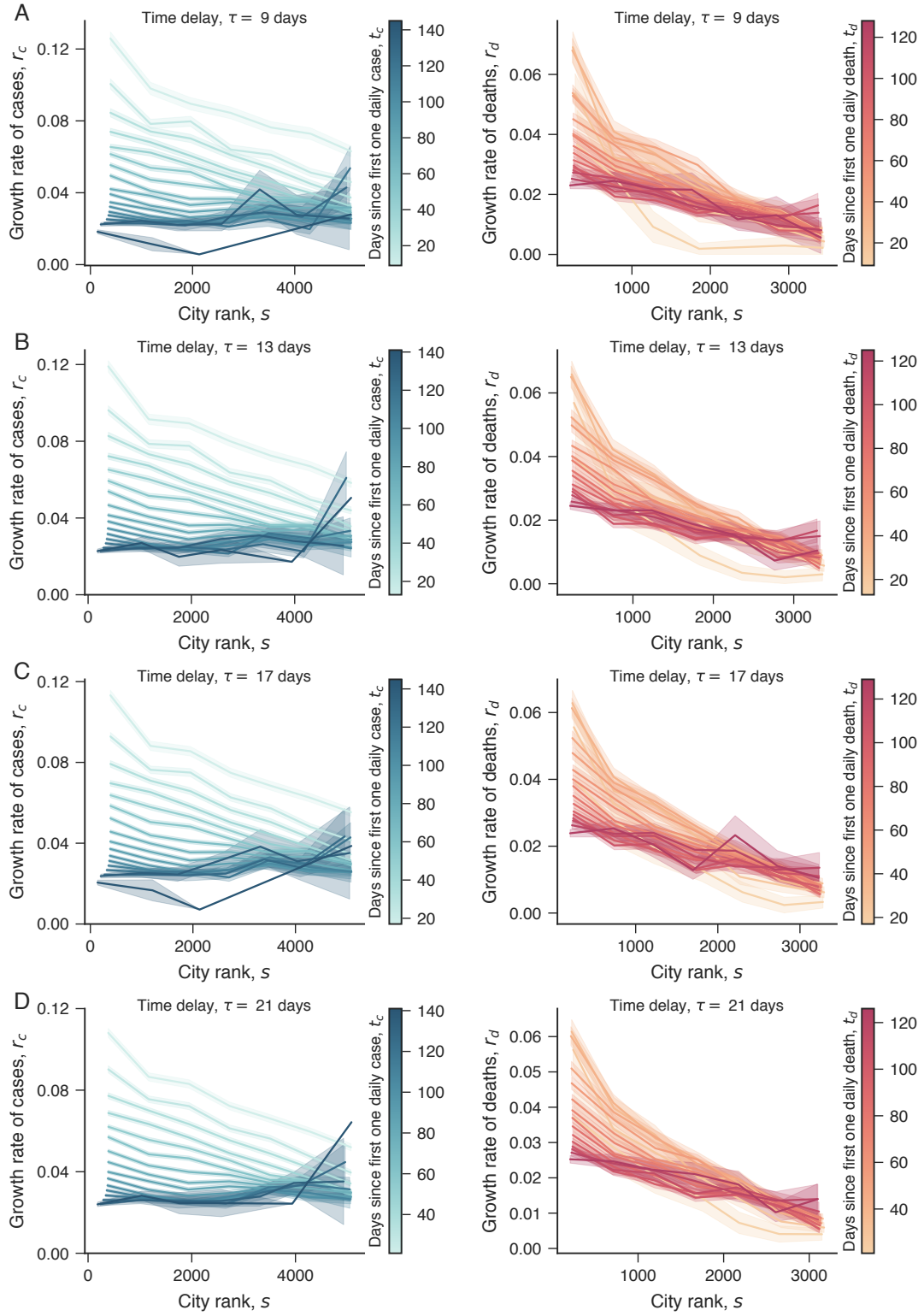


Figure 32. **Variations in the association between the growth rates and the city rank under different values of time delay τ .** Panels (A)-(D) show the average relationship between the growth rates of COVID-19 cases (r_c , left panels) and deaths (r_d , right panels) and the city rank s for number of days since the first one daily case (t_c) or death (t_d) and for different values of τ (indicated within the plots).

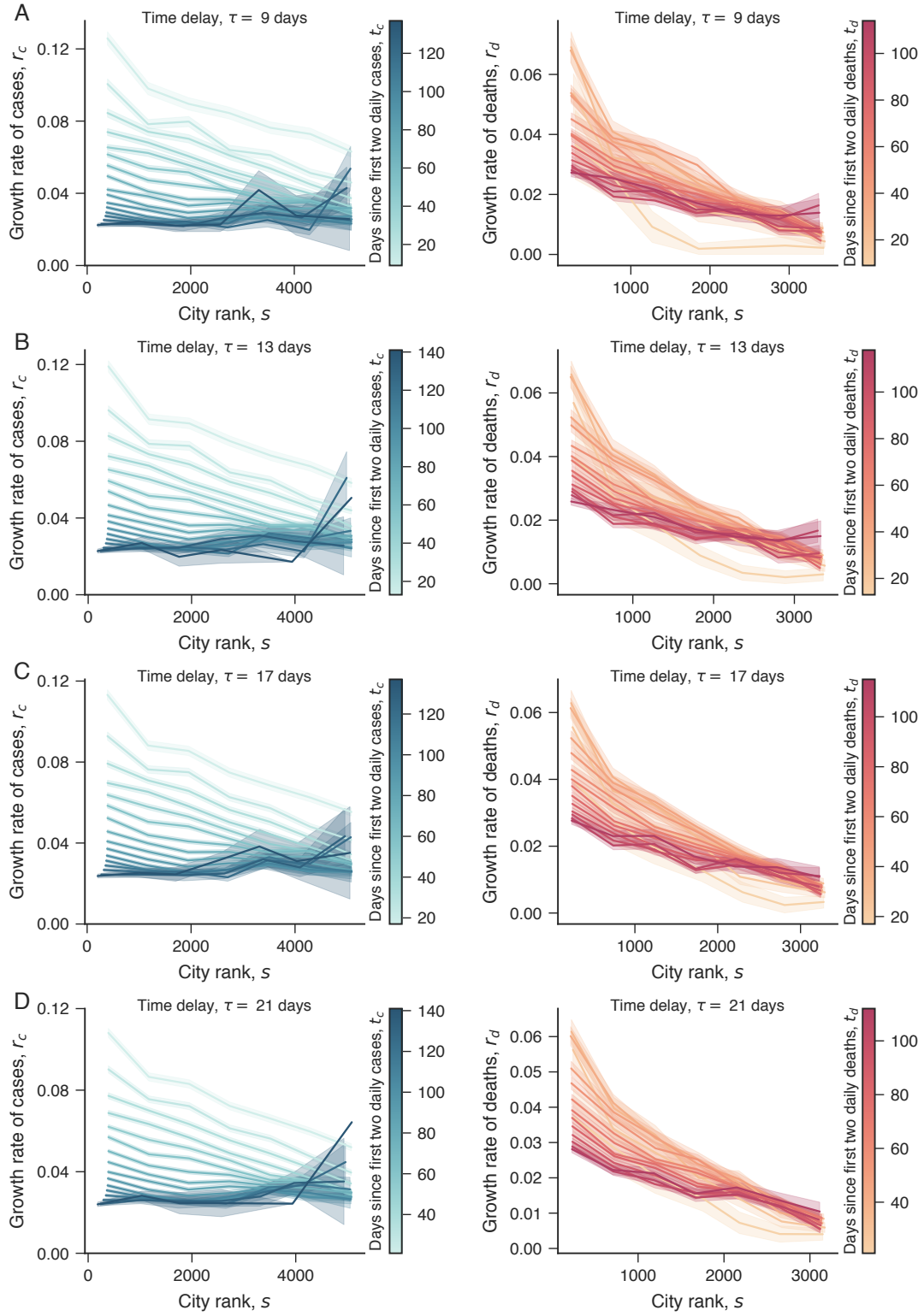


Figure 33. **Variations in the association between the growth rates and the city rank under different values of time delay τ .** Panels (A)-(D) show the average relationship between the growth rates of COVID-19 cases (r_c , left panels) and deaths (r_d , right panels) and the city rank s for number of days since the first two daily cases (t_c) or deaths (t_d) and for different values of τ (indicated within the plots).

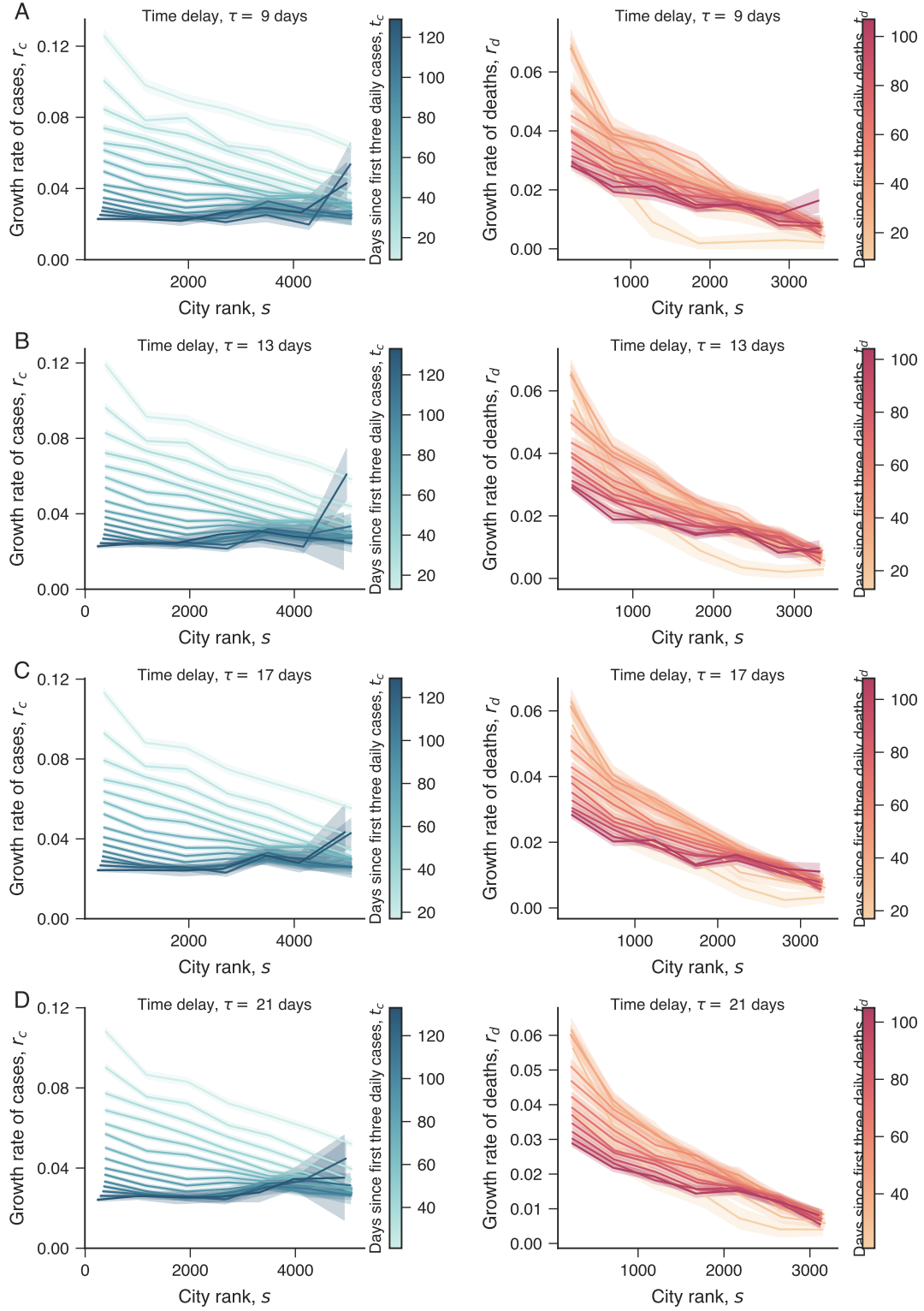


Figure 34. **Variations in the association between the growth rates and the city rank under different values of time delay τ .** Panels (A)-(D) show the average relationship between the growth rates of COVID-19 cases (r_c , left panels) and deaths (r_d , right panels) and the city rank s for number of days since the first three daily cases (t_c) or deaths (t_d) and for different values of τ (indicated within the plots).

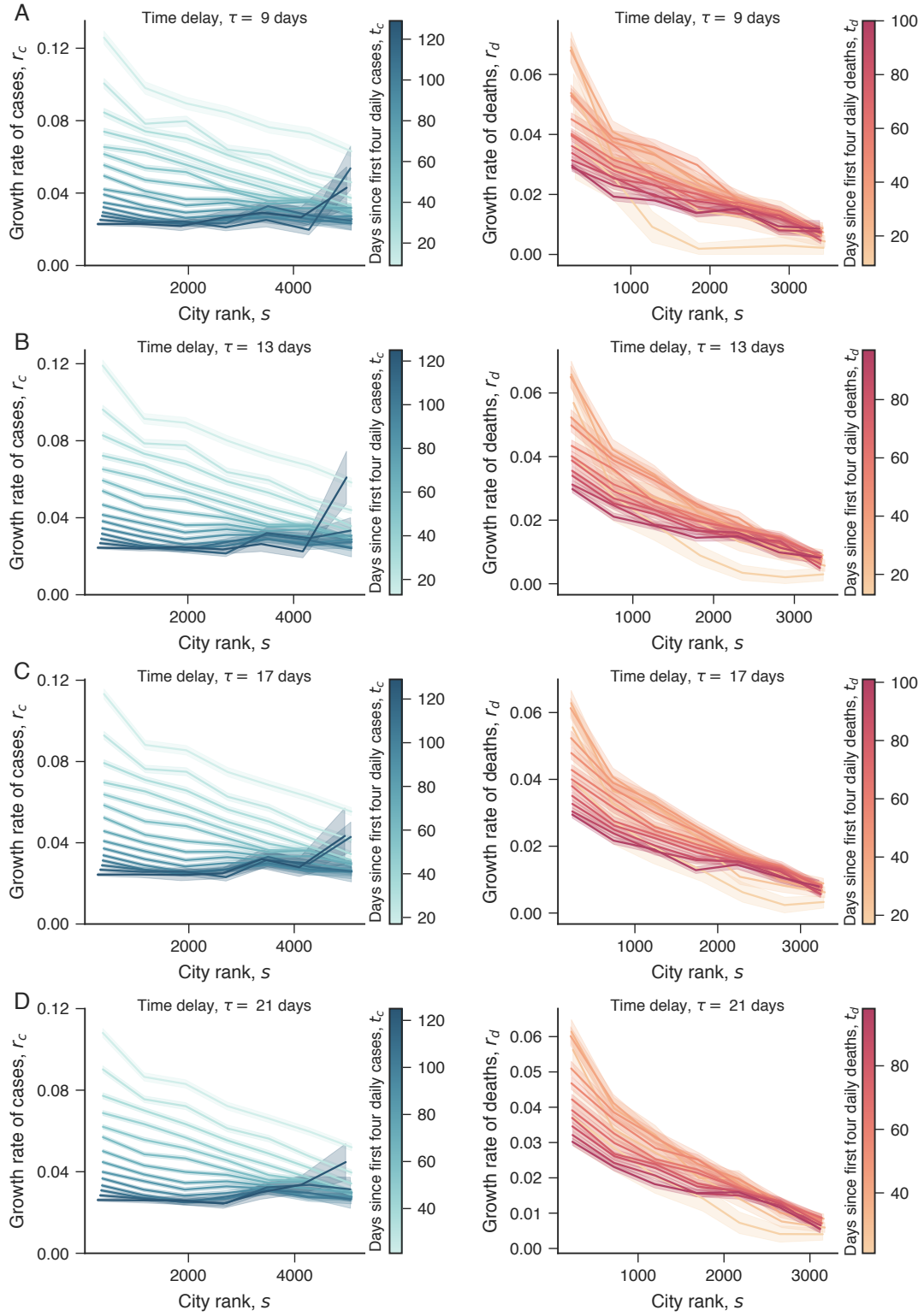


Figure 35. **Variations in the association between the growth rates and the city rank under different values of time delay τ .** Panels (A)-(D) show the average relationship between the growth rates of COVID-19 cases (r_c , left panels) and deaths (r_d , right panels) and the city rank s for number of days since the first four daily cases (t_c) or deaths (t_d) and for different values of τ (indicated within the plots).

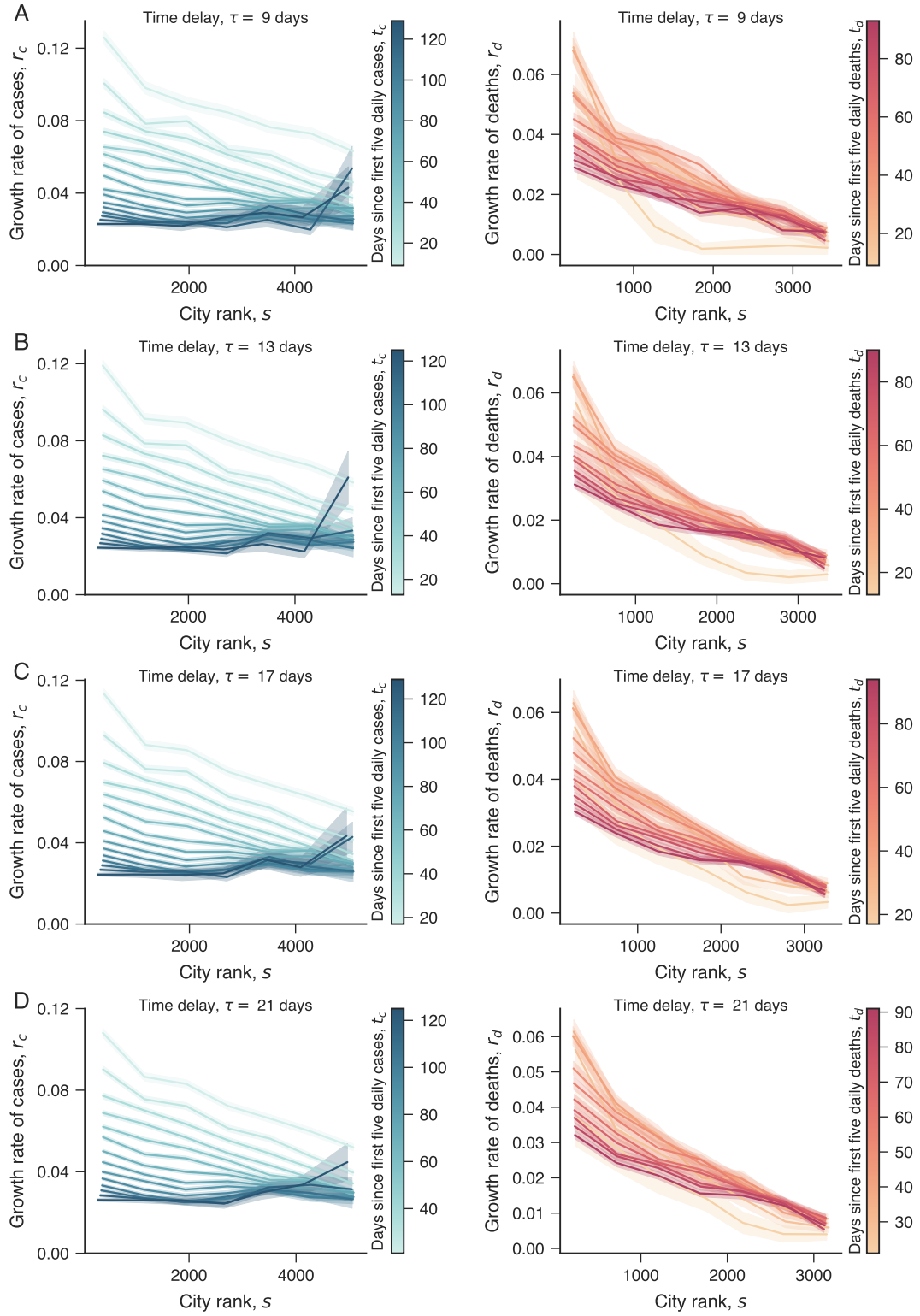


Figure 36. **Variations in the association between the growth rates and the city rank under different values of time delay τ .** Panels (A)-(D) show the average relationship between the growth rates of COVID-19 cases (r_c , left panels) and deaths (r_d , right panels) and the city rank s for number of days since the first five daily cases (t_c) or deaths (t_d) and for different values of τ (indicated within the plots).

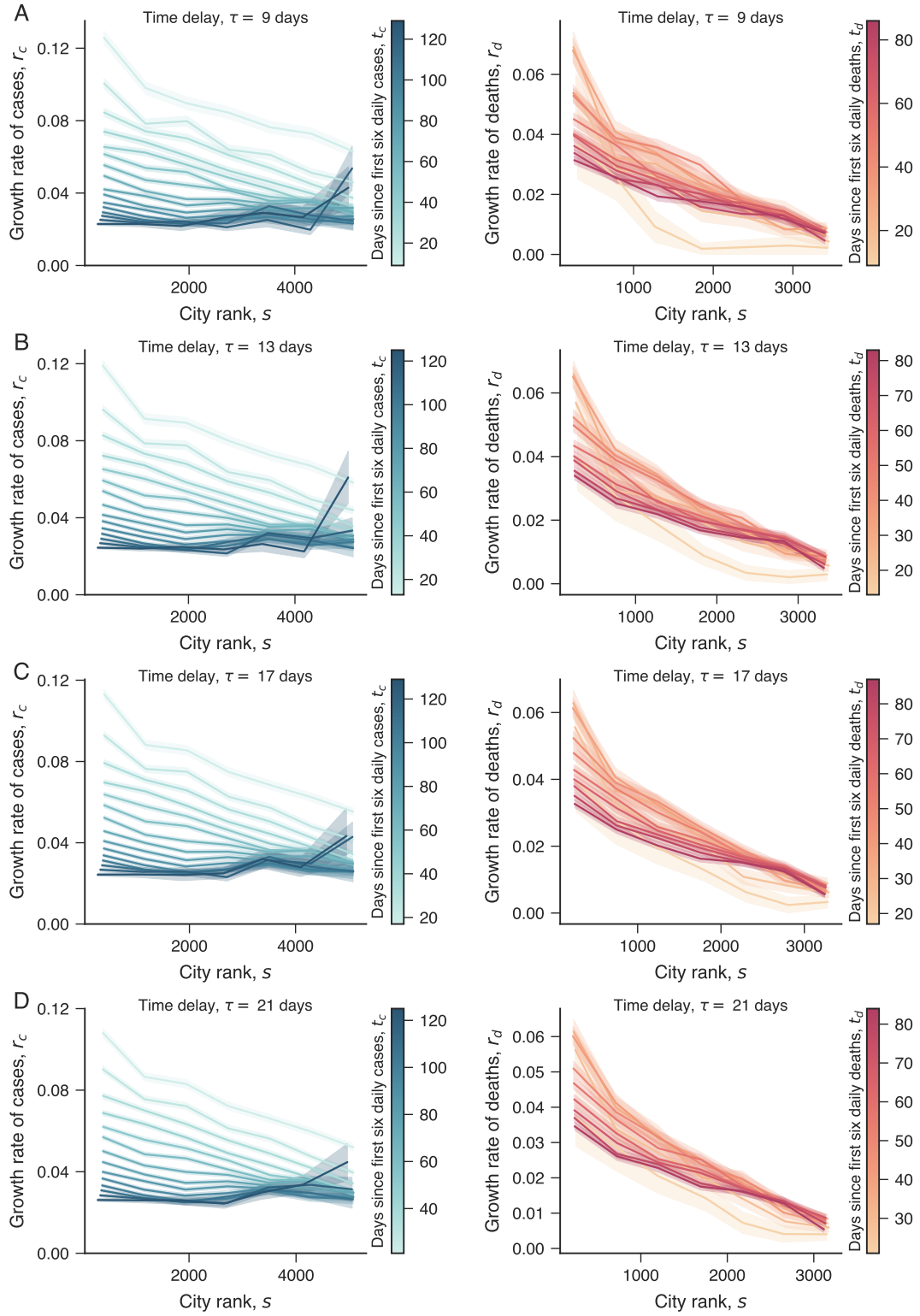


Figure 37. **Variations in the association between the growth rates and the city rank under different values of time delay τ .** Panels (A)-(D) show the average relationship between the growth rates of COVID-19 cases (r_c , left panels) and deaths (r_d , right panels) and the city rank s for number of days since the first six daily cases (t_c) or deaths (t_d) and for different values of τ (indicated within the plots).

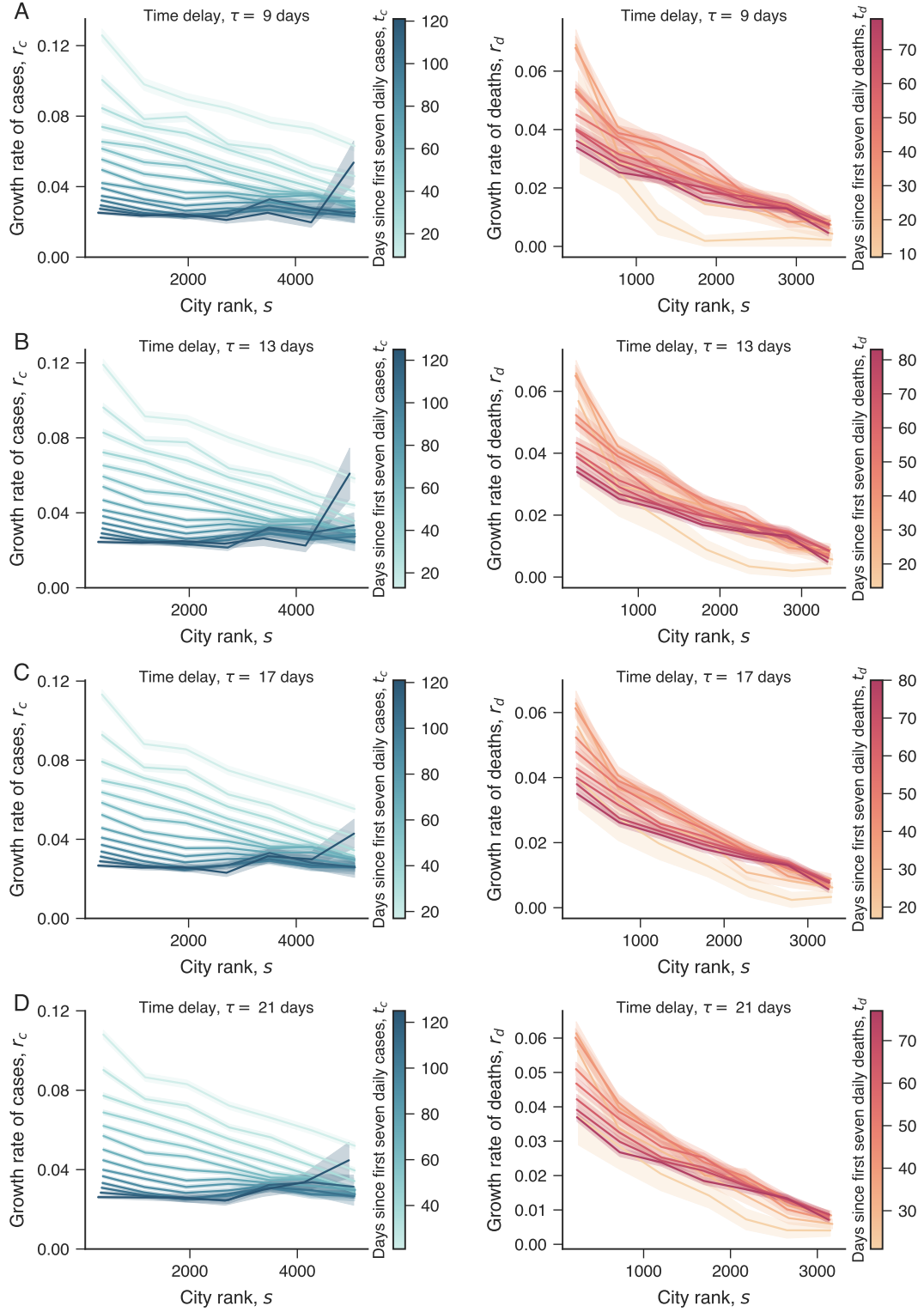


Figure 38. **Variations in the association between the growth rates and the city rank under different values of time delay τ .** Panels (A)-(D) show the average relationship between the growth rates of COVID-19 cases (r_c , left panels) and deaths (r_d , right panels) and the city rank s for number of days since the first seven daily cases (t_c) or deaths (t_d) and for different values of τ (indicated within the plots).